PNNL-11896
UC-602

Pacific Northwest National Laboratory

Operated by Battelle for the
U.S. Department of Energy

Drying Results of K-Basin Fuel Element 1164M (Run 6)

B. M. Oliver
G. S. Klinger
J. Abrefah
S. C. Marschman
P. J. MacFarlan
G. A. Ritter

August 1998

Prepared for the U.S. Department of Energy
under Contract DE-AC06-76RLO 1830

PNNL-11896

DISCLAIMER

PACIFIC NORTHWEST NATIONAL LABORATORY
operated by
BATTELLE
for the
UNITED STATES DEPARTMENT OF ENERGY
under Contract DE-AC06-76RLO 1830

Printed in the United States of America

Available to DOE and DOE contractors from the Office of Scientific and Technical Information, P.O. Box 62, Oak Ridge, TN 37831; prices available from (615) 576-8401.

Available to the public from the National Technical Information Service, U.S. Department of Commerce, 5285 Port Royal Rd., Springfield, VA 22161


This document was printed on recycled paper.
(9/97)

PNNL-11896
UC-602

Drying Results of K-Basin Fuel Element 1164M (Run 6)

B. M. Oliver
G. S. Klinger
J. Abrefah
S. C. Marschman
P. J. MacFarlan
G. A. Ritter

August 1998

Prepared for
the U.S. Department of Energy
under Contract DE-AC06-76RLO 1830

Pacific Northwest National Laboratory
Richland, Washington 99352

Summary

An N-Reactor outer fuel element that had been stored underwater in the Hanford 100 Area K-West Basin was subjected to a combination of low- and high-temperature vacuum drying treatments. These studies are part of a series of tests being conducted by Pacific Northwest National Laboratory on the drying behavior of spent nuclear fuel elements removed from both the K-West and K-East Basins.

The drying test series was designed to test fuel elements that ranged from intact to severely damaged. The fuel element discussed in this report was removed from K-West canister 1164M in 1996 and has remained in wet storage in the Postirradiation Testing Laboratory (PTL, 327 Building) since that time This element was split along the length in several places and appeared to be slightly bowed. Both ends of the element appeared to be intact. K-West canisters can hold up to seven complete fuel assemblies, but, for the purposes of this report, the element tested here is designated as Element 1164M.

The drying test was conducted in the Whole Element Furnace Testing System located in G-Cell within the PTL. This test system is composed of three basic systems: the in-cell furnace equipment, the system gas loop, and the analytical instrument package. Element 1164M was subjected to drying processes based on those proposed under the Integrated Process Strategy, which included a hot drying step. The test cycles are listed below:

- Cold Vacuum Drying (CVD) at ~50°C under vacuum (~15 hr)
- Pressure Rise Test at ~50°C (~1 hr)
- Hot Vacuum Drying (HVD) for a total of ~67 hr (~24 hr at ~80°C, ~35 hr at ~80°C to ~400°C, and ~8 hr at ~400°C)
- System Cooldown to ~50°C (~52 hr)
- Post-Test Pressure Rise Test at ~50°C (~1 hr).

Prior to CVD, ~10 ml of water were added to the system in addition to the water already on the surface of the fuel element. Approximately 5 ml of water were observed in the condenser during the condenser pumpdown phase of CVD, in close agreement with that calculated over the same time period. Observed pressure rise during the post-CVD Pressure Rise Test was ~0.14 Torr/hr, well below the acceptance criterion of 0.5 Torr/hr. Similar to earlier tests, the source of the total pressure rise observed in the post-CVD test was only partially from residual moisture, suggesting that other sources of gas are responsible for some of the total pressure rise observed in that test. Approximately 0.4 mg of water was calculated to have been removed during the Pressure Rise Test. This water can likely be interpreted as coming from free water that was trapped and not completely removed during CVD.

Water removal during the three phases of HVD was ~ 0.7 g, ~0.2 g, and ~12 mg, respectively. Approximately 15 mg of water were released during post-HVD cooldown, indicating small residual quantities of water remaining even after the drying test was completed. Water released during HVD-1 is attributed largely to the release of water from regions beneath the cladding and from under the corroded regions, with some release possibly from decomposition of metal oxy-hydrates. Water release peaks were observed during HVD-2 at ~130°C, ~176°C, and ~258°C. Water release during HVD-2 is probably from chemisorbed sites (i.e., hydrated species) at higher temperatures. As observed in previous drying tests, a temperature above 400°C may be required for complete drying of the fuel element within a reasonable period of time.

Hydrogen was observed during the test from both the mass spectrometer (MS) and gas chromatograph (GC) systems. Hydrogen was first observed at the beginning of HVD-1, reaching a peak at ~0.2 Torr·l before slowly decreasing. Approximately ~17 mg of hydrogen were released during HVD-1, attributed largely to oxidation of the fuel by remaining free water. Hydrogen release increased again during HVD-2, with two noticeable peaks at ~155°C (~22 mg) and ~260°C (~460 mg). The first peak roughly corresponds to a similar water release and is likely due to oxidation of fuel by water released through oxy-hydrate decomposition. The second release peak at ~260°C is likely due to uranium hydride decomposition. Above ~260°C, the level of hydrogen decreased rapidly, with only ~1.4 mg of hydrogen being released during HVD-3.

Total hydrogen release during HVD was ~500 mg. The level of hydrogen release for Element 1164M is the highest observed to date, and is approximately six times that observed for the previous element (6603M, Run 5). The level of hydrogen tends to support the suggestion of a high effective surface area due to a high degree of fuel fracturing. Hydrogen data from the MS showed the same general trends as the GC data. Xenon release occurring slightly after the large hydrogen release at ~260°C suggests some oxidation of newly exposed uranium underneath the uranium hydride that had decomposed.

Quality Assurance

This work was conducted under the Quality Assurance Program, Pacific Northwest National Laboratory (PNNL) SNF-70-001, *SNF Quality Assurance Program*, as implemented by the PNNL *SNF Characterization Project Operations Manual*. This QA program has been evaluated and determined to effectively implement the requirements of DOE/RW-0333P, Office of Civilian Radioactive Waste Management *Quality Assurance Requirements and Description (QARD)*. Compliance with the QARD is mandatory for projects that generate data used to support the development of a permanent High-Level Nuclear Waste repository. Further, the U.S. Department of Energy has determined that the testing activities which generated the results documented in this report shall comply with the QARD. Supporting records for the data in this report are located in the permanent PNNL SNF Characterization Project records, *Furnace Testing of SNF Fuel Element 1164M*.

Contents

Figures

Tables

Acronyms

ATS	Applied Test Systems
CVD	Cold Vacuum Drying
DACS	data acquisition and control system
DP	dew point
ET	elapsed time
GC	gas chromatograph
HP	Hewlett Packard
HVD	Hot Vacuum Drying
ID	inside diameter
IPS	Integrated Process Strategy
MS	mass spectrometer
NIST	National Institute of Standards and Technology
OD	outside diameter
PNNL	Pacific Northwest National Laboratory
PTL	Postirradiation Testing Laboratory
QA	Quality Assurance
QARD	Quality Assurance Requirements and Description
SFEC	single fuel element canister
SNF	spent nuclear fuel
UHP	ultra high purity
VP	vapor pressure

1.0 Introduction

The water-filled K-Basins in the Hanford 100 Area have been used to store N-Reactor spent nuclear fuel (SNF) since the 1970s. Because some leaks in the basin have been detected and some of the fuel is breached due to handling damage and corrosion, efforts are underway to remove the fuel elements from wet storage. An Integrated Process Strategy (IPS) has been developed to package, dry, transport, and store these metallic uranium fuel elements in an interim storage facility on the Hanford Site (WHC 1995). Information required to support the development of the drying processes, and the required safety analyses, is being obtained from characterization tests conducted on fuel elements removed from the K-Basins. A series of whole element drying tests (reported in separate documents, see Section 8.0) have been conducted by Pacific Northwest National Laboratory (PNNL)[(a)] on several intact and damaged fuel elements recovered from both the K-East and K-West Basins.

This report documents the results of the sixth of those tests, which was conducted on an N-Reactor outer fuel element removed from K-West canister 1164M. This element (referred to as Element 1164M) was stored underwater in the K-West Basin from 1983 until 1996. Element 1164M was subjected to a combination of low- and high-temperature vacuum drying treatments that were intended to mimic, wherever possible, the fuel treatment strategies of the IPS. The system used for the drying test was the Whole Element Furnace Testing System, described in Section 2.0, located in the Postirradiation Testing Laboratory (PTL, 327 Building). The test conditions and methodologies are given in Section 3.0. Inspections of the fuel element before and after the test are provided in Section 4.0. The experimental results are provided in Section 5.0, and discussed in Section 6.0.

(a) Operated by Battelle for the U.S. Department of Energy under Contract DE-AC06-76RLO 1830.

2.0 Whole Element Furnace Testing System

A complete description for the Whole Element Furnace Testing System, including detailed equipment specifications, is provided in Ritter et al. (1998).

2.1 Major Systems Overview

An overview of the furnace testing system is presented in this section. The subsystems pertinent to this test report are as follows:

- Vacuum Pumping System - This system consists of a scroll-type vacuum pump, a condenser with chiller, filters, valves, and piping, which provide the vacuum pressures and flows required for the proposed IPS vacuum processes.

- Process Heating System - This system consists of a resistively-heated, clam-shell furnace and a sample chamber (retort) to provide heating to the fuel element and to control process temperatures.

- Gas Supply/Distribution System - This system consists of gas bottles; mass flow controllers; piping; and valves for metering argon, air, or oxygen through the system. A bubbler is also available for adding water vapor to the system if desired.

- Gas Analysis Instrumentation - The gas analysis instrumentation includes a 300-amu quadrupole mass spectrometer (MS) and a gas chromatograph (GC) for monitoring selected elements in the process gas stream.

- Process Instrumentation - The system is equipped with several instruments for measuring process temperatures, pressures, and moisture level. An auxiliary turbo vacuum pumping system provides low system pressures for zero adjustment of the high accuracy retort pressure sensor.

- Data Acquisition and Control System (DACS) - The DACS consists of an IBM-compatible computer and data acquisition/control unit to monitor/store key system parameters (temperatures, pressures, flows, moisture level), along with controlling the process heating system and a safety argon system.

Figures 2.1 and 2.2 are photographs of the equipment located inside and outside of G-Cell. The furnace (including retort) and some of the process piping, instrumentation, and valves are located inside the hot cell. The furnace sits on the cell floor, and the process piping is routed to a rack that hangs on the west cell wall. Process piping, electrical power, and instrumentation wires pass through several split plugs on the west side of the cell. The process piping on the outside of the cell is contained within a glove bag, which provides a secondary containment as a precaution in case the

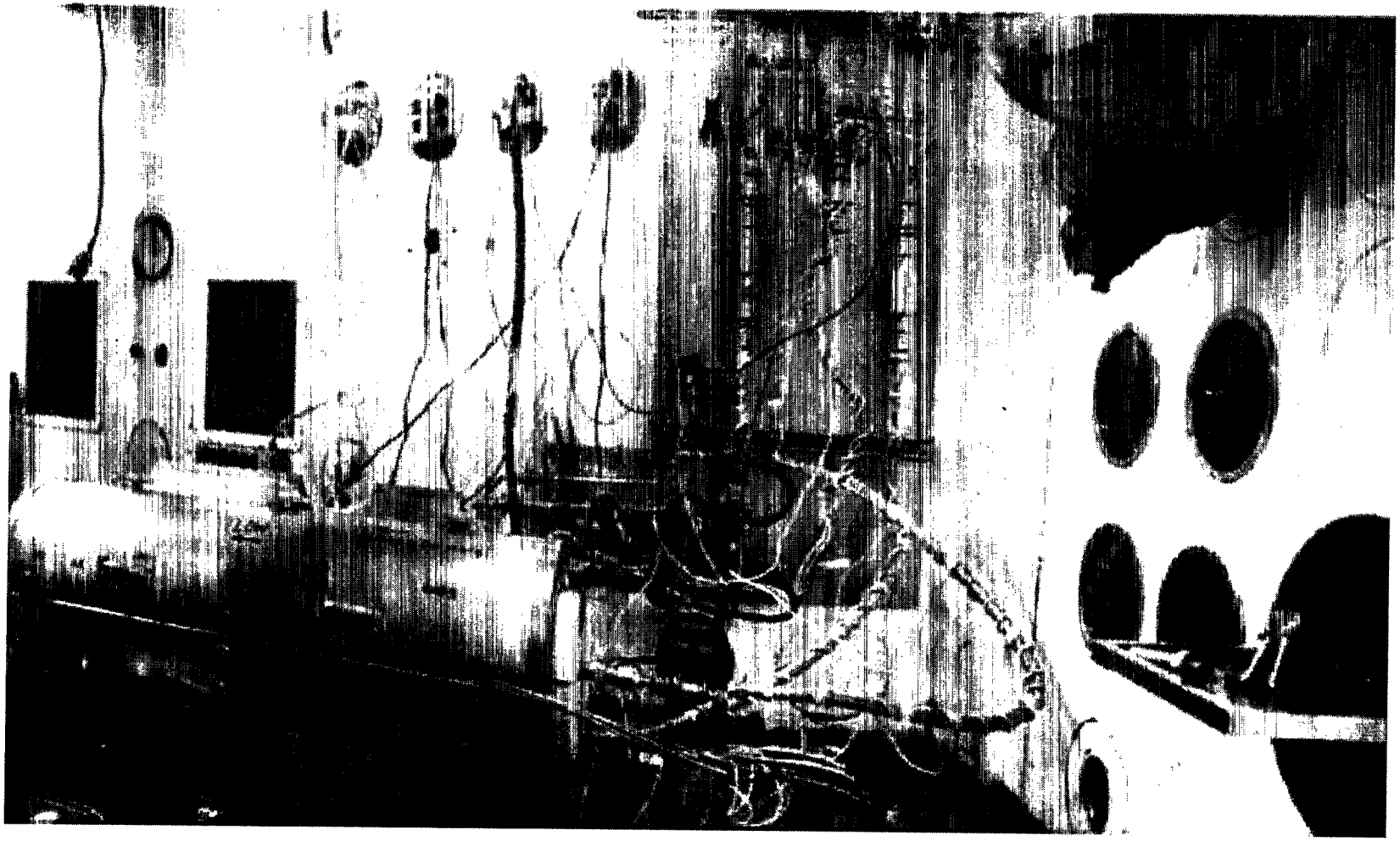

Figure 2.1. Fuel Element Drying System Components (in-cell)

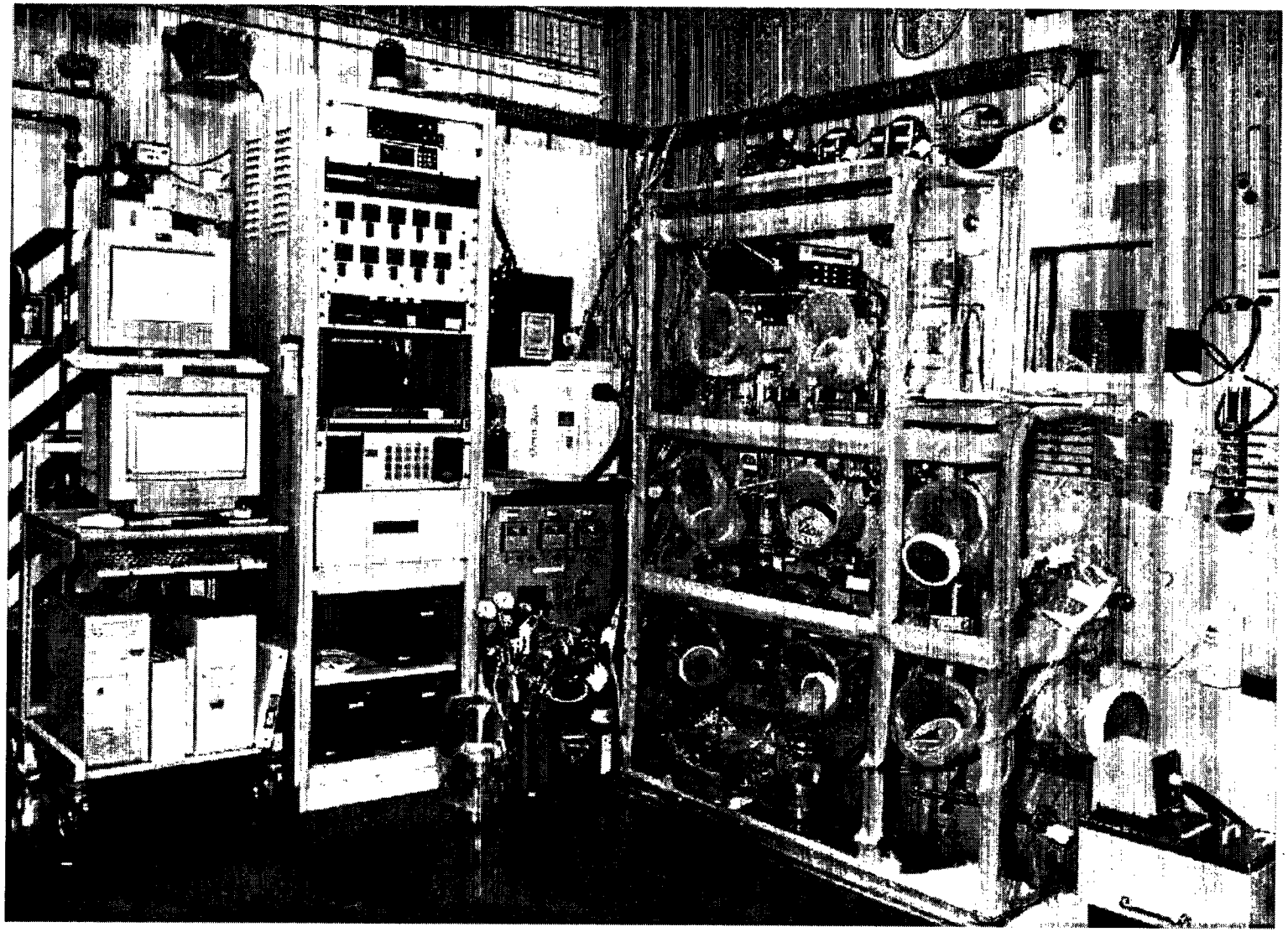

Figure 2.2. Fuel Element Drying System Components (ex-cell)

process piping lines become contaminated. The vacuum pump, condenser, bubbler, GC, and the remainder of the instrumentation and valves are located inside this glove bag. Instrumentation and electrical power wires are routed through pass-through sleeves on the sides of the glove bag to the instrument rack and computer console.

The instrument rack contains the readout/control units for the pressure sensors, moisture sensor, and flow controllers, along with the heat trace temperature controllers, data acquisition/control unit, turbo pump controller, GC laptop computer, and uninterruptible power supplies. The computers for the DACS and MS are located next to the instrument rack. The following sections provide more detailed descriptions of the components for these subsystems.

2.2 Vacuum Pumping System

The vacuum pumping system provides the pressures and flows required for the proposed IPS processes. This system connects the furnace retort with all the other components of the test system through various valves, fittings, and piping. The vacuum pumping system consists of the following components:

- scroll pump for evacuating the system to pressures below 1 Torr
- water condenser with refrigerated chiller for gross removal of water
- valves and piping for connecting the various components and controlling the flow direction
- particulate filters to prevent the spread of contamination
- heating cords with temperature controllers for preventing condensation in lines.

2.2.1 Varian Scroll Pump

The system vacuum pump is a Varian model 300DS scroll pump. This pump has an ultimate vacuum pressure less than 10^{-2} Torr and a peak pumping speed of 250 l/min (8.8 cfm). These pressures and flows are more than adequate for simulating the conditions of the proposed IPS vacuum processes. For a single fuel element, this amount of flow may be more than desired. Therefore, a metering valve was installed on the pump inlet to throttle the flow to lower levels as required. The desired system pressure is achieved by either using the metering valve or flowing ultra high purity (UHP) argon into the system through the entire gas loop or via a direct injection of ballast gas at the pump inlet. The use of argon gas helps to prevent the in-leakage of moisture-containing air through small system leaks (which are difficult to eliminate) that would interfere with process monitoring equipment.

2.2.2 Water Condenser

The scroll vacuum pump can be damaged by condensation of liquid water in the scroll mechanism, and, since each element was wet at the start of each test, the possibility of pump damage was considered. A water condenser with corresponding chiller was installed in the system to condense the bulk of the water before it reaches the pump. This condenser can be valved into the system in series with the scroll vacuum pump or can be bypassed if not needed. The condenser cannot trap all the liberated free water, but is efficient at removing the majority of free water in the system. The condenser is only used during the first phase of a Cold Vacuum Drying (CVD) test for a single fuel element. The condenser was custom fabricated specifically for this system. Detailed sketches and specifications for the condenser are given in Ritter et al. (1998).

2.2.3 Piping, Valves, and Filters

The vacuum pumping system connects the system components through various valves, fittings, and piping. A simplified piping schematic for the system is shown in Figure 2.3. This schematic shows the basic flow path of gases through the system that was used for this test, along with the relative locations of the major components, valves, and instruments. Detailed system piping diagrams are provided in Ritter et al. (1998), along with approximate lengths for the piping lines. As seen in Figure 2.3, there are numerous valves in the system that are used to direct the flow to and from the various components. Most of the valves in the system are ball valves and range from 1/4 in. to 1/2 in. nominal size. The system piping is constructed of thin wall tubing (1/4 in. to 1/2 in. OD) and is typically connected using simple Swagelok fittings (tees, elbows, unions, etc.). Ports for gas sampling/analysis and monitoring of system pressure, temperature, and humidity are also provided at key locations in the system piping. Special fittings and pipe-threaded fittings are used in some locations for connecting piping to the process instruments.

Particulate filters are installed in the system on both the inlet and outlet to the retort to help prevent the spread of contamination to the system piping on the outside of the hot cell. These filters are constructed of a microporous fiberglass media in a stainless steel housing. They are 99.9% efficient for particulates that are 0.2 microns and larger in size. Two different size filters, manufactured by Matheson, are used in the system.

2.2.4 System Line Heaters

All of the stainless steel tubing that carries gases into the furnace retort and resultant gases from the retort is heated to about 75°C to ensure condensable water vapor remains in the gas phase. Simple heat "cords" capable of being wrapped upon each other (as required at tees, elbows, and other connections) were found to be a good heating method for this system. The heating cords are controlled by simple proportional controllers. Type-K thermocouples are installed on each heated line so the DACS can be used to monitor and record temperature.

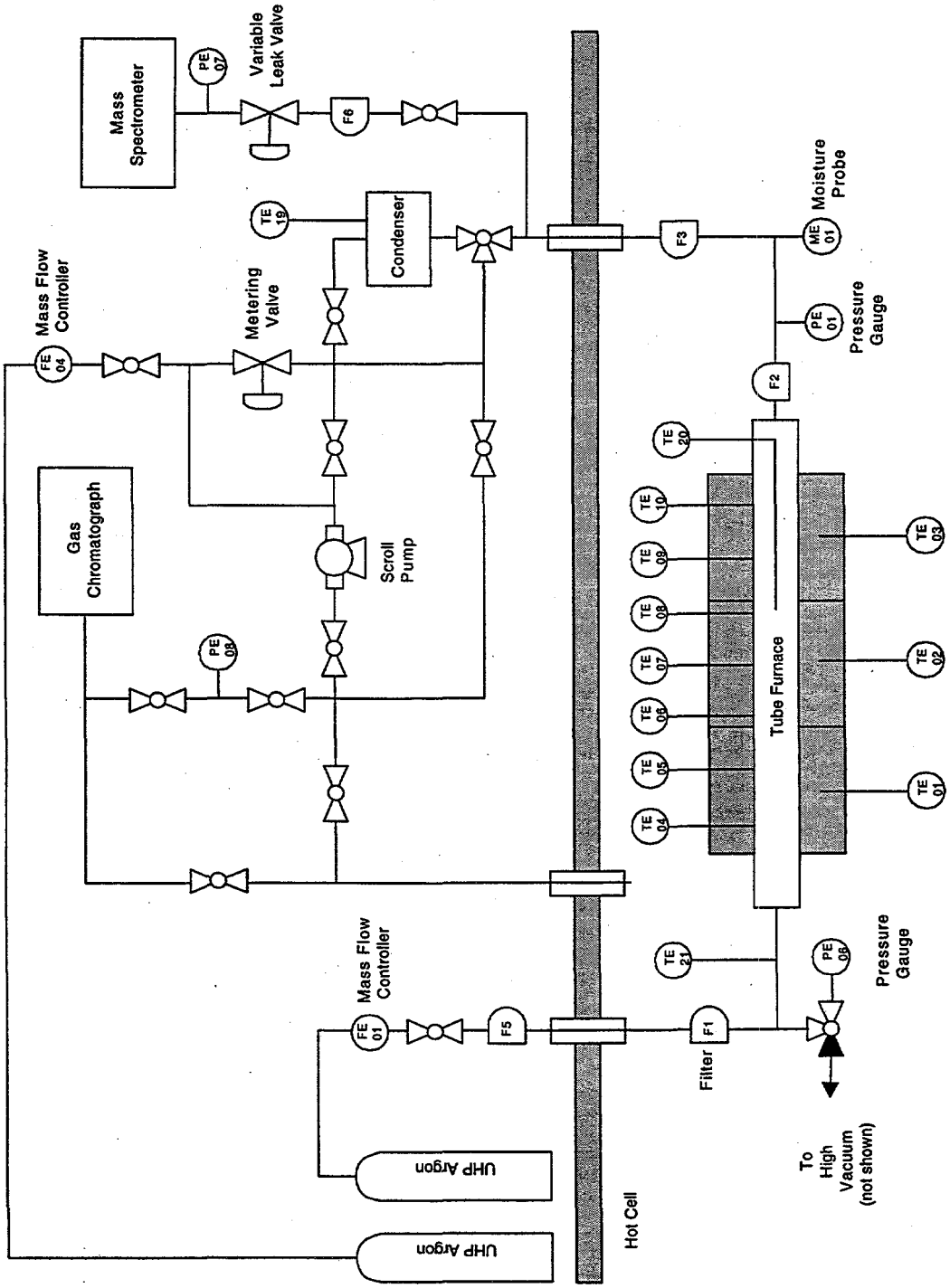

Figure 2.3. Generalized View of Test System

2.3 Process Heating System

The whole element furnace is a 4-ft-long, resistively-heated, clam-shell furnace. The furnace, a Series 3210 supplied by Applied Test Systems (ATS), has a temperature rating of 900°C and total heating capacity of 13,800 W. The internal dimensions are 5 in. ID by 45 in. long. The furnace has three separate sets of heating elements that allow the heating to be controlled in zones; each zone is 15 in. long and supplies up to 4600 W heating. The zones can be controlled separately to establish a flat temperature profile within the furnace, even though heat is lost preferentially out the end with the retort entry flange. A heat reflector consisting of several thin Inconel plates is used to reduce heat loss from the flange end of the retort. The furnace controller is an ATS Series 3000, which consists of three programmable, self-tuning proportional with integral and derivative controllers. These controllers are also interfaced to the DACS, which is capable of providing limited input to the controllers as required.

The retort, an ATS Series 3910, is an Inconel tube fitted with a gas inlet tube at one end and a gasketed flange at the other. Of all high-temperature materials, Inconel series 600 was selected to reduce the amount of oxidation and water pickup by the retort and associated components. Experience has shown that stainless steel components were easily affected by corrosion, which could then affect test results. The body of the retort is fabricated from schedule 40 Inconel pipe (4.5 in. OD, 4.026 in. ID), and the inside length is about 44.5 in. Seven type-K thermocouples are installed equidistant along one side of the retort and extend into the retort interior approximately 1/8 in. These thermocouples are used to monitor the retort temperature so that if a reaction with the fuel element occurs (which would locally raise the retort temperature), this event can be correlated with the approximate location on the fuel.

An Inconel sample/transfer boat is used to load the fuel element into the furnace. The boat is fabricated from an 11-gauge (0.120-in.-thick) Inconel 601 sheet, which is formed into a flattened u-shape. The boat has a weir and a swivel handle on each end. The weirs are used to keep free water or particulates contained in the boat as required.

2.4 Gas Supply/Distribution System

The gas supply system and vacuum pumping system together are capable of controlling the fuel element environment to vacuum or moderate pressure conditions, and/or exposing the fuel element to a variety of gases or gas mixtures. The gas loop is typically operated as a single-pass system with no capability for recirculation. The gas supply system consists of gas bottles; mass flow controllers; piping; and valves for metering argon, air, or oxygen through the system. A bubbler is also available for adding water vapor to the process gas stream as required, but it was not used in these tests.

The gas supply system contains three Matheson mass flow controllers calibrated for argon, air, and oxygen. All gases are typically specified "ultra high purity" and are additionally filtered for water using molecular sieve columns. Argon is the principal inert gas used, as it is more dense than air; provides reasonable thermal conductivity; and requires simpler handling procedures than lighter gases such as helium. The argon purge gas is introduced into the retort through FE-01, which is a Matheson model 8272-0422 oxygen controller, recalibrated for argon gas at 25°C using a NIST-traceable bubble flow meter. The recalibration resulted in a flow rate range of 0 - 324 sccm argon. Air and oxygen are not

currently used because any oxidative steps have been deleted from the current IPS for the SNF. The manufacturer's specifications for the air and oxygen controllers' flow rate ranges are 0 - 1000 sccm air and 0 - 10 sccm oxygen. If higher flow rates are desired, a new mass flow controller with a higher range could be procured and installed in the system.

2.5 Gas Analysis Instrumentation

2.5.1 Balzers Omnistar Mass Spectrometer

The Balzers Omnistar MS is a compact, computer-controlled, quadrupole MS capable of scanning to 300 amu. The unit is capable of monitoring up to 64 components within a gas stream with a nominal detection limit of less than 1 ppm for most gases other than hydrogen. The MS was used to monitor hydrogen, nitrogen (for air in-leakage), krypton, xenon, and other elements during the test.

The MS was modified as a result of early system testing and calibration to improve the time response to small changes in hydrogen pressure. Before testing, the MS was calibrated for hydrogen using mixtures of hydrogen and helium, and hydrogen and argon gas. The residence time of each gas could be measured in the quadrupole chamber, and it was observed that the hydrogen decay time was approximately four times as long as helium. This was not unexpected as turbomolecular pumps have a lower pumping efficiency for very light gases. In standard practice this is acceptable, but for these tests, where determining hydrogen could be very important, steps were taken to improve the hydrogen decay time. The MS vacuum system was modified by adding a stainless steel flanged tee, a gate valve, and a room-temperature hydrogen getter downstream from the quadrupole. Under vacuum, the gate valve can be opened, exposing the getter to the system to help scavenge hydrogen from the system following analysis. This modification reduced the residence time of hydrogen in the system substantially, and decreased the background level of hydrogen by about a factor of 2. The getter improved the system response to transient events that might result in the release of hydrogen.

A Granville-Phillips variable leak valve, series 203, was added to the gas sampling inlet of the MS to permit operation over a wide range of system pressures. Without the leak valve, system pressures above about 40 Torr produce too much flow through the MS capillary tube, which overwhelms the turbo pump used to pump down the MS vacuum chamber. Flow through the leak valve can be continuously varied from 0.4 l/s to 10^{-11} l/s, which allows the MS inlet pressure to be controlled to any pressure desired, even if the system pressure varies dramatically. The pressure on the low-pressure side of the leak valve is measured using a Cole-Parmer sensor (PE-07) and recorded by the DACS. The inlet head pressure is divided by the pressure used for the calibration, and this factor is applied to the test data for calculating actual gas concentrations. Prior to the present test, the MS was calibrated at ~30 Torr head pressure with two certified gas standards consisting of 114 and 1050 ppmv hydrogen in argon.

2.5.2 MTI M200 Gas Chromatograph

The MTI M200 Gas Chromatograph is a high-speed GC that is used to monitor the quantities of hydrogen and other light gases in the furnace testing system gas loop. This instrument is interfaced with a laptop computer to record data. The GC is designed to operate at near-atmospheric pressure; thus, it may

be configured in two different ways for measurement purposes. At system pressures near atmospheric, the GC is configured to sample directly from the gas loop ahead of the system vacuum pump. When the system is under vacuum, the GC is configured to sample from the exhaust side of the vacuum pump. The gas output from the pump is sufficiently compressed that the GC can sample and analyze this gas. The GC inlet pressure is measured using a Cole-Parmer pressure sensor (PE-08) and recorded by the DACS. No correction for the difference in the sample pressure and calibration pressure is applied, since both are ~760 Torr (1 atm). The GC was calibrated using three certified gas standards consisting of 11, 114, and 1050 ppmv hydrogen.

2.6 Process Instrumentation

The furnace testing system contains several process instruments for monitoring moisture content, pressure, and temperature. The key instruments are as follows:

- Panametrics moisture monitor
- MKS Baratron pressure transducers
- Cole-Parmer pressure transducers
- Type-K thermocouples.

2.6.1 Panametrics Moisture Monitor

The Panametrics moisture monitor model MMS35 uses a solid electrochemical probe (model M2L) that measures moisture by measuring the characteristic capacitance of the probe as a function of the moisture in the gas phase. The sensor has a nominal dew point range of -110°C to 20°C. Previous testing indicated that contamination by radioactive elements (e.g., cesium) causes the probe to lose calibration and results in moisture readings that drift with time. To prevent contamination of the probe tip, the probe is installed in the gas loop downstream of two glass particulate filters. Further, the probes are changed following each test and surveyed for radioactive contamination. If no contamination is found, and the data correlate well with the data obtained from the MS, the readings are accepted.

A calibration verification procedure can be performed using calibrated water "leak" tubes. These tubes can be placed inside the furnace and, when heated, will establish a known water vapor pressure in the system. However, this procedure is time intensive; approximately 2 weeks are required to calibrate one probe over the range of moisture likely to be encountered in these tests. This procedure is only used if the moisture monitor results vary widely from the MS data.

Output of the moisture monitor is in dew point (DP) in degrees Celsius. For comparison with other test data, these dew point values were converted to water vapor pressure in Torr using the water and ice vapor pressure data shown in Table 2.1. Interpolation of the data was accomplished using a 6th-order polynomial fit to the log of the vapor pressure (VP) versus temperature data. The resulting conversion expression is as follows:

Table 2.1. Water and Ice Vapor Pressure Data Versus Temperature

Dew Point (°C)	Vapor Pressure (VP)		
	(Pa)[a]	(Torr)	Log (Torr)
-80	5.500E-02	4.126E-04	-3.385E+00
-75	1.220E-01	9.151E-04	-3.039E+00
-70	2.610E-01	1.958E-03	-2.708E+00
-65	5.400E-01	4.051E-03	-2.392E+00
-60	1.080E+00	8.101E-03	-2.091E+00
-55	2.093E+00	1.570E-02	-1.804E+00
-50	3.936E+00	2.952E-02	-1.530E+00
-45	7.202E+00	5.402E-02	-1.267E+00
-40	1.284E+01	9.631E-02	-1.016E+00
-35	2.235E+01	1.676E-01	-7.756E-01
-30	3.801E+01	2.851E-01	-5.450E-01
-25	6.329E+01	4.747E-01	-3.235E-01
-20	1.033E+02	7.746E-01	-1.109E-01
-15	1.653E+02	1.240E+00	9.339E-02
-10	2.599E+02	1.950E+00	2.899E-01
-5	4.018E+02	3.014E+00	4.791E-01
0	6.113E+02	4.585E+00	6.614E-01
10	1.228E+03	9.212E+00	9.644E-01

(a) CRC Press. 1997. *Handbook of Chemistry & Physics*, 78th edition.

$$VP\ (Torr) = \log^{-1}[C_1 \cdot DP^6 + C_2 \cdot DP^5 + C_3 \cdot DP^4 + C_4 \cdot DP^3 + C_5 \cdot DP^2 + C_6 \cdot DP + C_7] \quad (2.1)$$

where $C_1 = -6.7260E-12$
$C_2 = -1.7250E-09$
$C_3 = -1.7089E-07$
$C_4 = -7.2618E-06$
$C_5 = -2.9668E-04$
$C_6 = 3.4414E-02$
$C_7 = 6.5933E-01$

2.6.2 MKS Baratron Pressure Transducers

Two MKS Baratron model 690 calibrated pressure transducers coupled with MKS model 270 signal conditioners are used as the primary measurement for the overall system pressure. As shown in Figure 2.3, PE-01 measures the system pressure downstream of the retort outlet, whereas PE-06 measures the system pressure at the retort inlet. PE-01 indicates pressure in the range of 0.1 Torr to 10,000 Torr. The pressure range of PE-06 is 0.01 Torr to 1000 Torr. PE-06 was installed after the first two fuel element drying tests to provide more accurate measurements than PE-01 for low pressures. PE-06 is

therefore considered the primary system pressure measurement. In addition, the 270 signal conditioner procured with PE-06 has a special capability to remotely zero the transducer, which provides more accurate pressure measurements below 1 Torr.

An auxiliary high vacuum turbo pump is used to evacuate the inlet to PE-06 to well below 10^{-4} Torr, so that the transducer can be accurately re-zeroed. The 270 signal conditioner used with PE-01 does not have a remote zeroing capability. Both signal conditioners have analog outputs that are interfaced to the DACS so that system pressure is continuously recorded.

2.6.3 Cole-Parmer Pressure Transducers

Two Cole-Parmer model H-68801-53 diaphragm-type, calibrated pressure transducers are installed on the MS and GC sample lines as indicated by PE-07 and PE-08 in Figure 2.3. These pressure measurements are used to normalize the MS and GC data so that actual gas concentrations in the system can be calculated from the relative concentrations measured. These sensors have a range of 0 to 1500 Torr with a resolution of 0.1 Torr, and an accuracy of ±1% or ±1 Torr, whichever is larger. Both readout units (model H-68801-03) have analog outputs that are interfaced to the DACS so that these pressures are continuously recorded.

2.6.4 Thermocouples

Thermocouples provide a simple, reliable method for measuring system temperatures. As shown in Figure 2.3, over 20 thermocouples are installed at various locations in the system to provide key temperature measurements. The retort temperatures are of primary importance, and these temperatures are measured by thermocouples TE-04 through TE-10, which are positioned equidistant along the length of the retort. Other key temperature measurements include the retort center temperature (TE-20, which is a 30-in.-long thermocouple installed through the outlet end of the retort); retort inlet temperature (TE-21); condenser gas temperature (TE-19); and the condenser coolant temperature (TE-22). Thermocouples TE-11 through TE-17 are used for controlling the temperature of the heated lines. All thermocouple readings are continuously recorded using the DACS.

2.7 Data Acquisition and Control System

The DACS monitors system parameters and controls the furnace and the safety argon system. The DACS consists of a Hewlett Packard (HP) 3497A data acquisition/control unit, and an IBM-compatible computer. A National Instruments general purpose interface bus card, installed in the IBM-compatible computer, is used to communicate with the HP 3497A. The computer communicates with the furnace temperature controllers over serial port 0 using an RS-232/RS-485 converter. The DACS uses National Instruments LabView for Windows as the control software.

The DACS is designed to measure critical system parameters during fuel conditioning tests, including temperatures, pressures, flow rates, and moisture level. The measured parameters are converted to engineering units, displayed on the computer screen, and stored to disk at user-defined intervals. The data

files are stored in a tab-delimited format to allow importing into a standard spreadsheet or plotting program. A plotting screen also allows for plotting of up to six parameters at a time.

Limited control of the furnace can be performed with the DACS. Each of the three furnace zone temperatures can be remotely set by the DACS. In addition, the DACS allows the operator to start and stop the furnace and select one of four temperature profiles that are pre-programmed in the furnace temperature controllers. Note that these profiles must be programmed manually in the furnace controllers before using the DACS to select them.

3.0 Vacuum Drying Testing of Element 1164M

The drying test was performed in accordance with Test Procedure, *Furnace Testing of N-Reactor Fuel Element 1164M*, PTL-007, Revision 0. This document is located in the PNNL permanent project records for this test.

The testing consisted of three parts (discussed in this section):

- removing the fuel from its shipping canister, performing a visual inspection, loading the fuel onto the furnace system sample boat, and transferring it to the PTL G-Cell for loading into the furnace.
- drying the fuel element using a combination of Cold Vacuum Drying (CVD) and Hot Vacuum Drying (HVD) processes.
- unloading the furnace, performing a post-test visual inspection, and returning the fuel element to its shipping canister.

3.1 Fuel Element Transfer and Loading

3.1.1 Pre-Test Visual Inspection

The pre-test visual inspection was conducted using a high-resolution color CCD video camera located inside the PTL F-Cell (adjacent to G-Cell), where the sample was unloaded from the shipping canister and visually inspected. The results were recorded using a Panasonic Super-VHS resolution video recorder. This examination was conducted to document the condition of the fuel element prior to the test and to determine if any changes had occurred since it was removed from the K-West Basin and shipped to the PTL. The results of this inspection are presented in Section 4.0.

3.1.2 Fuel Element Rinsing

Fuel element 1164M had been stored in the PTL water storage pool contained in a single fuel element canister (SFEC) that was filled with K-Basin water. Before the start of the drying test, the element was rinsed in F-Cell. This rinsing involved raising and lowering the element several times in the SFEC using one of the cell's manipulators. Following rinsing, the element was transferred to G-Cell for loading into the element test retort.

3.2 Fuel Element Drying

The fuel element was subjected to cold and hot vacuum drying. The drying test was conducted in six phases:

1. Cold Vacuum Drying
2. Pressure Rise Test
3. Hot Vacuum Drying (first step)
4. Hot Vacuum Drying (second step)
5. Hot Vacuum Drying (third step)
6. Post-Test Pressure Rise Test.

The nominal design conditions used for these test phases are summarized in Table 3.1. Each phase is discussed below.

Table 3.1. Summary of Nominal Test Design Conditions

Test Segment	Nominal Test Condition[a]
A. Cold Vacuum Drying	
System Configuration	Pump on,[b] argon gas flow during initial condenser pumpdown phase
Test Temperature, °C	50
Atmosphere	Vacuum
Pressure, Torr	<5
Gas Flow Rate, cc/min	0
Gas Species Monitored	H_2, H_2O, N_2, O_2, CO_2, Ar, Kr, Xe
Duration, hr	CVD is conducted until the total pressure in the retort falls below 0.5 Torr.
B. Pressure Rise Test	
System Configuration	Test Chamber Isolated
Test Temperature, °C	50
Atmosphere	Vacuum
Initial Pressure, Torr	<5
Gas Flow Rate, cc/min	0
Gas Species Monitored	H_2, H_2O, N_2, O_2, CO_2, Ar, Kr, Xe
Pressure Rise (acceptable level, Torr)	<0.5
Duration, hr	1
C. Hot Vacuum Drying (Step 1)	
System Configuration	Pump on,[b] argon gas flow
Test Temperature Range, °C	75
Atmosphere	Vacuum, Ar background
Pressure, Torr	15
Gas Flow Rate, cc/min	300
Gas Species Monitored	H_2, H_2O, N_2, O_2, CO_2, Ar, Kr, Xe
Duration, hr	24

Table 3.1. (contd)

Test Segment	Nominal Test Condition[a]
D. Hot Vacuum Drying (Step 2)	
System Configuration	Pump on,[b] argon gas flow
Test Temperature Range, °C	75 to 400
Temperature Ramp Rate, °C/hr	10
Atmosphere	Vacuum, Ar background
Pressure, Torr	15
Gas Flow Rate, cc/min	300
Gas Species Monitored	H_2, H_2O, N_2, O_2, CO_2, Ar, Kr, Xe
Duration, hr	35
E. Hot Vacuum Drying (Step 3)	
System Configuration	Pump on,[b] argon gas flow
Test Temperature, °C	400
Atmosphere	Vacuum, Ar background
Pressure, Torr	15
Gas Flow Rate, cc/min	300
Gas Species Monitored	H_2, H_2O, N_2, O_2, CO_2, Ar, Kr, Xe
Duration, hr	10
F. Cooldown	
System Configuration	Pump on,[b] argon gas flow
Test Temperature, °C	400 to 50
Atmosphere	Vacuum
Initial Pressure, Torr	15
Gas Flow Rate, cc/min	300
Gas Species Monitored	H_2, H_2O, N_2, O_2, CO_2, Ar, Kr, Xe
Duration, hour	~100
G. Pressure Rise Test	
System Configuration	Test Chamber Isolated
Test Temperature, °C	50
Atmosphere	Vacuum
Initial Pressure, Torr	<5
Gas Flow Rate, cc/min	0
Gas Species Monitored	H_2, H_2O, N_2, O_2, CO_2, Ar, Kr, Xe
Duration, hour	1

(a) Nominal test design conditions. Actual values are given in the text.
(b) Vacuum pump was throttled during the drying test.

3.2.1 Cold Vacuum Drying

While the fuel element was being handled and prepared for the drying test, it was kept damp by sprinkling it with deionized water. The amount of surplus liquid water, though small, could not be ascertained. There were no pools of water in the sample boat; however, water was adsorbed into corroded areas, cracks, and crevices. Just before loading it into the furnace, an additional ~10 ml of water were added to the sample boat to ensure sufficient free water in the system prior to CVD.

The furnace was first purged with argon to remove as much air as possible. The furnace was then isolated and the furnace temperature increased to approximately 50°C and allowed to stabilize. After stabilization, argon flow was re-established; the system vacuum pump was turned on (in a throttled mode); and the system water condenser valved in. When the system pressure became lower than the condenser could extract, the condenser was valved out of the gas loop and the argon flow stopped. The remainder of the CVD was conducted with the throttled vacuum pump. CVD was conducted at an ultimate pressure of ~0.2 Torr for ~16 hr. The purpose of the CVD portion of the test was to determine if CVD is successful in removing the majority of the free water from the system in a reasonable length of time.

3.2.2 Pressure Rise Test

The Pressure Rise Test involved isolating the system and measuring any pressure increase while at CVD pressure and temperature conditions. The purpose of the Pressure Rise Test was to determine the effectiveness of the preceding CVD process. This test was conducted by valving the vacuum pump out of the gas loop and closing the exhaust valves. The condition for acceptance of this portion of the test is a total system pressure rise of less than 0.5 Torr in a 1-hr time period. If this condition is not met, the system is re-opened to the vacuum pump and the Pressure Rise Test repeated.

3.2.3 Hot Vacuum Drying, Step 1

Following completion of the Pressure Rise Test, the vacuum pump was re-opened to the system retort; argon gas flow was established at a rate of ~324 cc/min; and the retort temperature was increased to ~76°C. This condition was held for a period of ~25 hr. This portion of the test can be used to obtain isothermal hydrogen and water release data for assessing oxidation of the fuel at low temperatures.

3.2.4 Hot Vacuum Drying, Step 2

The second step of the HVD process involved raising the temperature of the retort from ~80°C to ~400°C at a carefully controlled rate while maintaining the same argon flow and pressure conditions. Thus, any release of gas species during this temperature rise could be assigned to a specific temperature. The second step of HVD was conducted for about 35 hr.

During this step, hydrogen may be released from the fuel through the decomposition of uranium hydride (Cotton 1988); this reaction is rapid at temperatures greater than 250°C:

$$UH_3 \rightarrow U + \frac{3}{2}H_2 \qquad (3.1)$$

Water may also be liberated by various hydrated species found on fuel elements, such as hydrates of uranium oxides, aluminum hydroxides, and hydrated iron oxides. Water is also released slowly along a "tortuous path" from beneath corroded parts of the fuel element and from behind the cladding. The released water can react with the fuel element to generate hydrogen through the reactions:

$$U + 2H_2O \rightarrow UO_2 + 2H_2 \tag{3.2}$$

$$UH_3 + 2H_2O \rightarrow UO_2 + \frac{7}{2}H_2 \tag{3.3}$$

3.2.5 Hot Vacuum Drying, Step 3

The final step of the HVD process involved holding the temperature of the retort at ~400°C while again maintaining the same argon flow and pressure conditions as in steps 1 and 2. This step will yield isothermal release data for any remaining hydrated species on the fuel element, and for oxidation of uranium by any remaining water. This final step of the HVD process was conducted for about 10 hr.

3.2.6 System Cooldown and Post-Test Pressure Rise Test

Following completion of the final HVD step, the system retort was allowed to cool to ~50°C, and then another Pressure Rise Test was conducted to determine the baseline in-leakage rate of air into the retort from the cell environment. Knowing this rate is important to allow for correction of the system and moisture pressure increase rates determined in the initial post-CVD Pressure Rise Test. Since the conditions for the post-HVD test are identical to those used for the initial test, the assumption is made that the air in-leakage rate should be nearly the same as well.

3.3 Calculation of Water and Hydrogen Inventories

Assuming ideal gas behavior of the water vapor, total water inventory (m) in the system during those portions of the test conducted with argon flowing into the retort can be approximated from the measured water vapor pressure and the argon gas flow as follows:

$$\frac{dm}{dt} = \frac{M}{V_0} \cdot \frac{P_w}{(P_t - P_w)} \cdot \frac{dV}{dt} \tag{3.4}$$

where dm/dt is the rate of water removal in grams per minute, M is the molecular mass of water in grams per mole, dV/dt is the flow rate in liters per minute (at the calibration temperature of 25°C), V_0 is the molar volume of gas at 25°C and 1 atmosphere in liters per mole, P_w is the partial pressure of water vapor in Torr, and P_t is the total pressure in Torr. The total amount of water released is given by integrating the rate data over time.

The hydrogen inventory may be calculated in a similar fashion with the $[P_w/(P_t - P_w)]$ expression in the above equation replaced with the measured atom fraction of hydrogen. For the purposes of this report, all hydrogen data are plotted in Torr·l rather than grams. At the calibration conditions of the argon flow controller, 1 Torr·l is equivalent to approximately 0.11 mg of hydrogen.

The assumptions made in estimating the water and hydrogen values are:

- The flow into the retort is approximately equal to the flow out (i.e., contributions to the flow from other gas species such as hydrogen are neglected).
- The argon mass flow is referenced to 25°C (as determined from the calibration of the flow gauges).
- The sample gas is at the same temperature as the calibration gas (GC and MS measurements).

4.0 Visual Examinations of Element 1164M

An N-Reactor fuel assembly consists of an inner element and outer element made from a uranium alloy co-extruded with a Zircaloy-2 cladding. Both elements are annular, right-cylinders. The inner element has a smaller outer diameter and is held in place within the outer element.

Fuel element 1164M, chosen for Run 6, was an outer element removed from the K-West Basin in 1996. The element had been in sealed water storage in the K-West Basin since 1983. This fuel element was selected to represent a classification of fuel damage termed "mid-cracks" (Lawrence 1997). The furnace drying test series (of which this is Run 6 of 8) were intended to progress from intact (unbreached) fuel elements to severely damaged fuel elements. This fuel element was to represent a fuel element in between those appearing to be only broken (as in Run 3) and those that are severely damaged (as in Run 7). Note: An as-fabricated N-Reactor outer element (Mark IVE) has the dimensions: 66.3 cm in length, 6.15 cm OD, 4.31 cm ID.

The fuel element had been kept in K-Basin water at the PTL storage basin since it was loaded into its SFEC and shipped to the facility in 1996. The first relatively detailed examination of the fuel element was conducted just before the drying test and is discussed below.

4.1 Pre-Test Visual Examination

The fuel element was removed from its SFEC and examined using a CCD color video camera in the PTL F-Cell. The fuel element was split along the length in several places and appeared to be slightly bowed; however, both ends of the element appeared to be intact. Figure 4.1 shows a composite of two frames captured from the visual examination video. The darkening around the cracks was due to water that wicked up from the interior of the fuel element. The cladding surfaces dried quickly (as has been the case with every fuel element examined), as the hot cell has high air flow and is warm due to the bright cell lighting.

Figure 4.2 shows two additional views of the fuel element. Again, the dark areas surrounding the cracks were due to water wicking up from the interior of those cracks. In places, the fuel cladding appeared to be separated from the uranium matrix, but no significant pieces of cladding were missing. Small fragments of fuel fell out of the element during the visual examination.

The element was slightly bowed along the length due to corrosion of the uranium matrix. The bow appeared to cause less than 5 mm of misalignment along the element length. Initially, it was thought the element might be broken and only held together by the cladding; however, this was discounted as the fuel element did not break apart during handling. The fuel element appeared to have a light coating on the surface, as on the fuel elements in drying runs 4 and 5 (Elements 5744U and 6603M, respectively). Similarly, attempts to collect the coating were unsuccessful because the material was too thin.

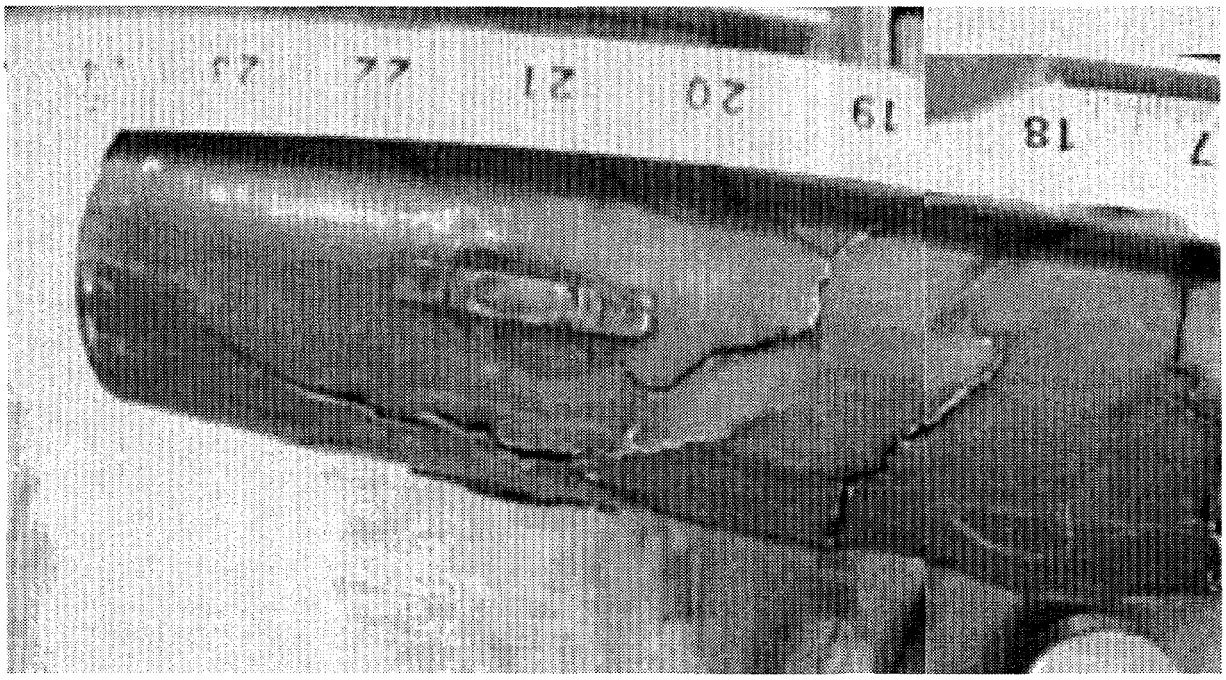

Figure 4.1. Composite View of Element 1164M Showing Several of the Surface Cracks

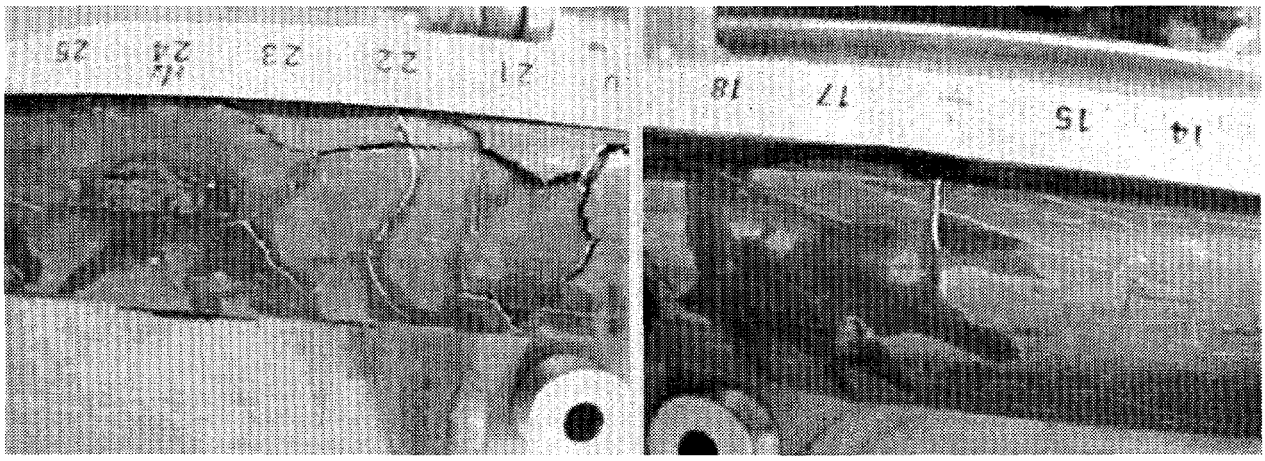

Figure 4.2. Two Pre-Test Views of Element 1164M Showing Additional Cracking and Water Wicking from the Interior of the Fuel Element

4.2 Post-Test Visual Examination

Similar to the fuel elements tested in Runs 4 and 5, the fuel element surface coloration changed from a light gray color to a dark color following the test. This could be due to the transformation of uranium oxy-hydrates releasing water and leaving behind simpler oxide phases. Some oxides are known to be dark in color. As noted, because the coating material is so thin, none of it could be recovered for analysis.

The fuel element cracks also were broadened as a result of the drying test. As discussed in Section 3.0, the drying process used for this test involved several stages, included a step during which the fuel element was heated to 400°C. Therefore, it is uncertain during which stage the cladding cracks opened further. It was possible to view the fuel matrix under the cladding cracks in many places. The fuel matrix had an appearance similar to shattered glass. This was different from the appearance of fuel elements 5744U and 6603M. The bulk fuel matrix in those tests had a more solid appearance with less fracturing.

Figures 4.3 and 4.4 show composite views of two areas of the fuel element. The view in Figure 4.3 allows the fuel matrix to be seen. Because the angle of the camera to fuel changed as the hot cell operator moved the camera along the fuel element length, the ruler measurements are somewhat inaccurate. The shattered appearance of the fuel matrix can be seen in the area where the cladding has pulled away from the fuel. This is an as-found view of the fuel element; the cladding was not physically pulled away for this picture. Figure 4.4 shows another region where the cracks broadened as a result of the drying process. Many of the cracks nearly traverse the circumference of the fuel element.

It was noted during the post-test examination that fuel fines and shards would fall out of the element each time it was rotated. Some of these fines are shown in Figure 4.5 lying beside or below the element. It was also noted that, although the fuel element had cracks that ran almost completely around the circumference, the element did not break into two or more pieces. However, the fuel element was handled carefully, and no attempts to test its integrity were made.

In addition to the fuel fines and shards, the view shown in the far right of Figure 4.5 is the same area of exposed fuel shown in Figure 4.3. In this view, the cladding "tab" that peeled back was removed to allow a closer inspection of the fuel matrix. The fuel cladding was very brittle; the tab snapping free with a single bend. The fracture surface appeared "granular," as would be expected from a brittle-type failure. The embrittlement may be due to hydriding of the cladding, but this is unconfirmed. The high degree of fuel fracture is also clearly evident in this view. This fuel element may also have a high effective surface area due to the high degree of fuel fracturing.

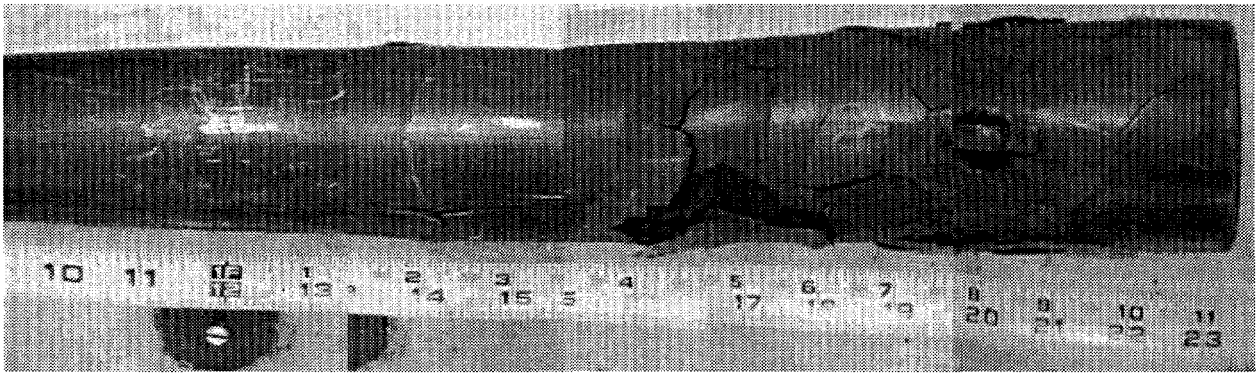

Figure 4.3. Post-Drying Composite View of Fuel Element 1164M

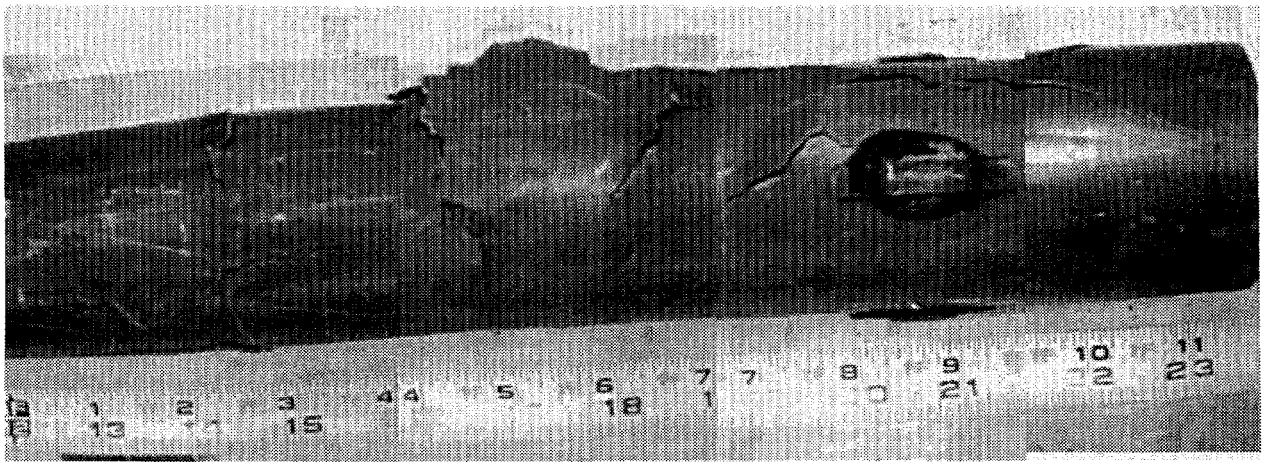

Figure 4.4. Post-Drying Composite View of Fuel Element 1164M Approximately 90° from the View Shown in Figure 4.3

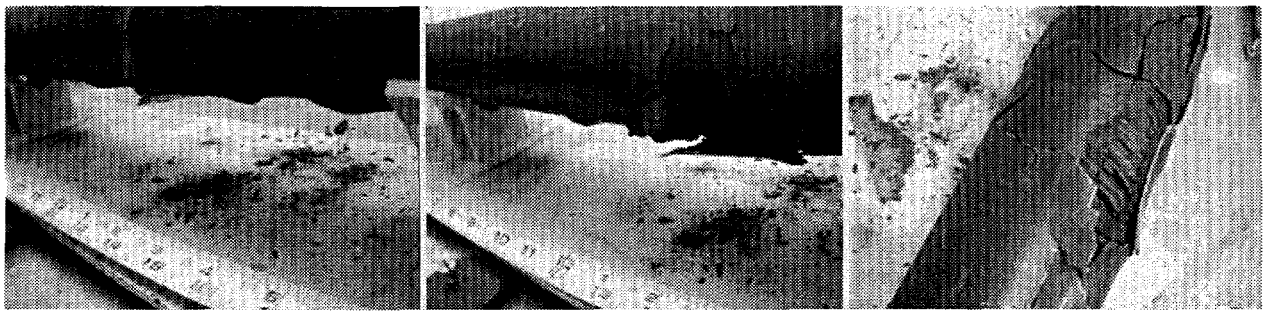

Figure 4.5. Three Views of Fuel Element 1164M Following the Drying Test. Small shards of fuel material can be seen in the background of the image.

5.0 Experimental Results

In the following sections, the experimental data collected during the drying test are expanded and plotted for each segment. Summary results from the test are plotted in Figure 5.1. This figure shows the system moisture level response to the pressure changes and the retort tube temperatures during the test. Time intervals for the various test segments are shown in the upper section of the plot, and are also outlined in Table 5.1. The temperatures shown in Figure 5.1 were recorded from one of seven thermocouples (TE-07) on the system located near the center of the retort. The pressure data were taken from the 0 to 1000 Torr Baratron sensor (PE-06) located upstream of the retort.

5.1 Cold Vacuum Drying

The water release from the CVD portion of the test is shown in Figure 5.2. The baseline moisture partial pressure in the system prior to heating was ~13 Torr at a retort temperature of ~24°C. Total system pressure was ~752 Torr, with no argon gas flow. After heating to ~50°C, the moisture pressure and system pressure stabilized at ~11 Torr and ~830 Torr, respectively. Based on the pressure differences at these two temperatures, and assuming ideal gas behavior, there is an approximately 12 Torr pressure difference. This pressure difference has been observed in all the previous tests, except for the first dry-run, and may have been due to gases evolved during the heatup, such as hydrogen from moisture reactions, and gases dissolved in the free water. Another explanation for the calculated pressure difference is that the average retort temperature was somewhat greater than 50°C.

The CVD phase started at an elapsed time (ET) of 230 min. Figure 5.2 shows that the moisture pressure rose almost immediately to ~14 Torr, and "saturated" at this pressure for about 50 min. This saturation behavior has been observed in previous tests, and is a result of the dew point exceeding the maximum of 20°C for the Panametrics moisture probe. At an ET of ~322 min, argon flow was stopped and the condenser was valved out. Pumping was continued by the throttled vacuum pump. By the end of CVD (ET = 1143 min), the moisture pressure had dropped to ~0.3 Torr, whereas the total pressure was indicating a slightly lower value at ~0.2 Torr. The reason for this apparent discrepancy is not clear, but may indicate the inherent combined accuracies of the Baratron and Panametrics sensors.

Approximately 5 ml of water were observed in the condenser during the CVD phase. Because of the design of the condenser, however, it is possible that the observed water is an underestimation of the total water collected. Calculated water removal during the time period when the condenser was open under argon flow, however, yielded a value of ~5 g, in close agreement with the observed water in the condenser. Approximately 10 ml of water were added at the start of the test, in addition to any water remaining on the element from the initial element rinsing.

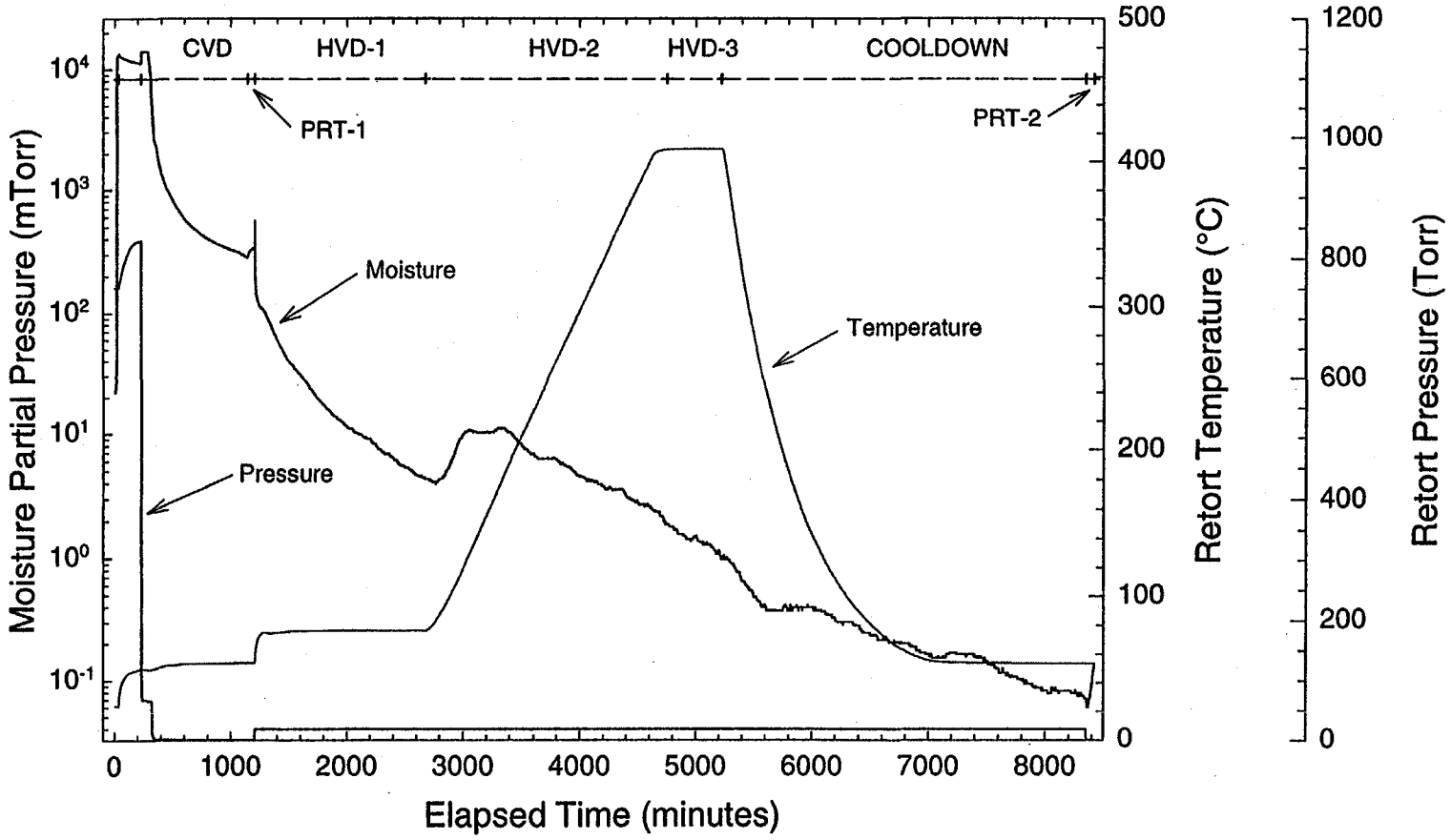

Figure 5.1. Drying of SNF Element 1164M, Summary Plot

Table 5.1. Fuel Element 1164M Drying Run Time Line

Activity	Date/Time	Elapsed Time (min)
Start of Test		
Heat furnace to ~50°C	01/20/98 13:44	36
Cold Vacuum Drying Test		
Open pump[(a)] and condenser (initial), start argon flow	01/20/98 16:58	230
Open pump, close condenser (final), stop argon flow	01/20/98 18:30	322
Pressure Rise Test		
Close pump (isolate furnace)	01/21/98 08:11	1143
Open pump valve	01/21/98 09:14	1206
Hot Vacuum Drying Test (Step 1)		
Start argon flow (~320 cc/min), raise furnace temperature to ~80°C and hold	01/21/98 09:15	1207
Hot Vacuum Drying Test (Step 2)		
Raise furnace temperature to ~400°C @ 10°C/min	01/22/98 09:45	2677
Hot Vacuum Drying Test (Step 3)		
Hold furnace temperature at ~400°C	01/23/98 20:25	4757
System Cooldown		
Reduce temperature of retort to ~50°C, maintain argon flow	01/24/98 04:11	5223
Post-Test Pressure Rise Test		
Turn off argon flow, and close pump valve (isolate furnace)	01/26/98 08:35	8368
Turn off furnace heaters, end test	01/26/98 09:28	8420
(a) The vacuum pump was throttled for the drying test.		

5.2 Pressure Rise Tests

The results of the two pressure rise phases of the drying test (post-CVD and post-HVD) are shown in Figures 5.3 and 5.4. As discussed earlier, the purpose of the post-HVD test was to determine as best as possible the ambient air in-leakage rate into the system as it had been configured for the drying test. While under vacuum conditions, with no argon flow, any air in-leakage will contribute to the data signals observed for the various process gases measured during the test, particularly water and hydrogen. The data plotted for the total pressure are from the 0 to 1000 Torr Baratron sensor (PE-06) located upstream of the retort. This sensor has higher sensitivity and therefore lower noise than the 0 to 10,000 Torr Baratron (PE-01) located downstream of the retort. To calculate total water mass removed from the retort, however, pressure data from the 0 to 10,000 Torr sensor were used, as this sensor is closer to the moisture sensor. Differences in the pressure indications of the two sensors nevertheless are small and therefore negligible when compared with overall system uncertainties.

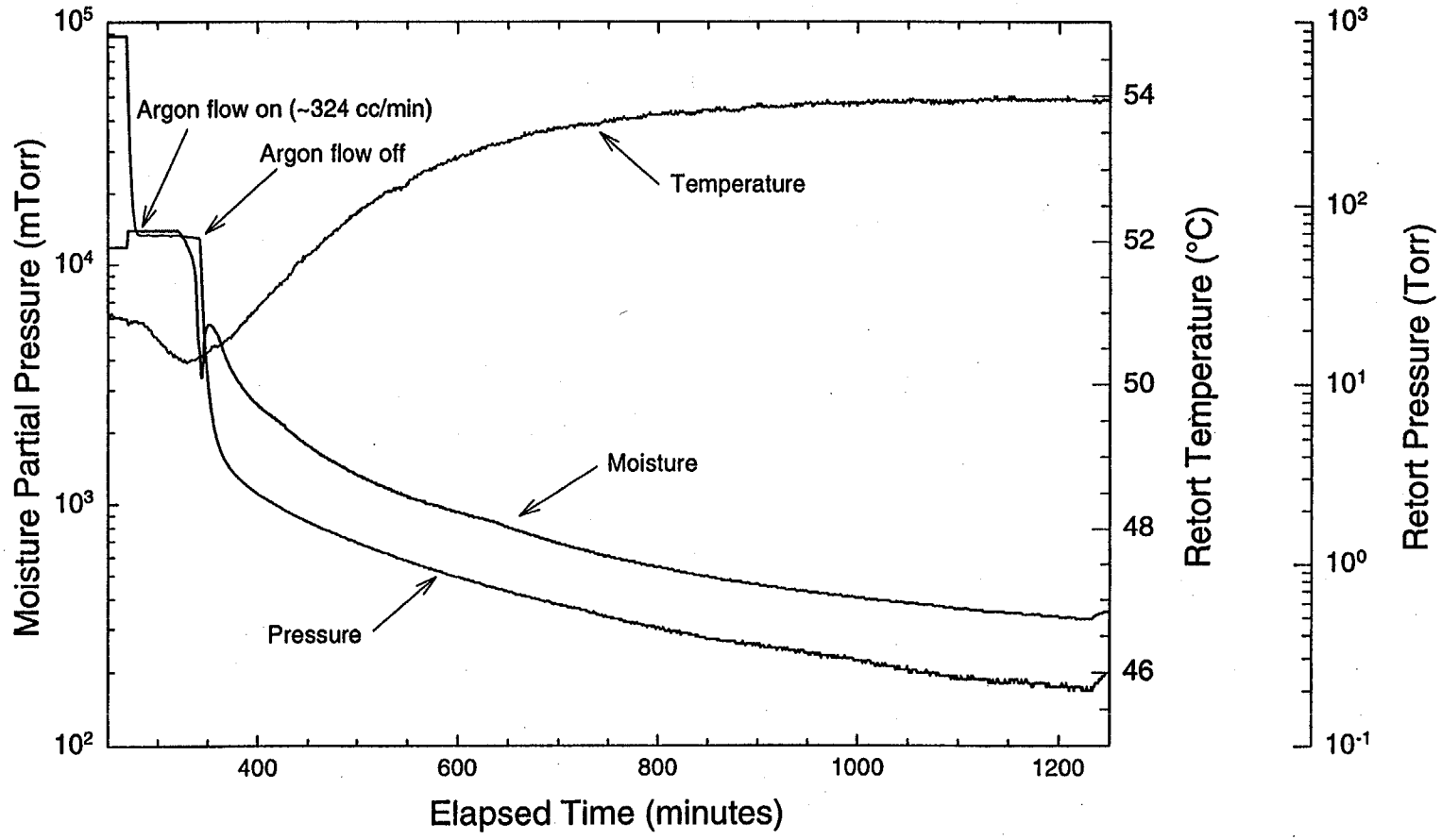

Figure 5.2. Drying of SNF Element 1164M, Cold Vacuum Drying

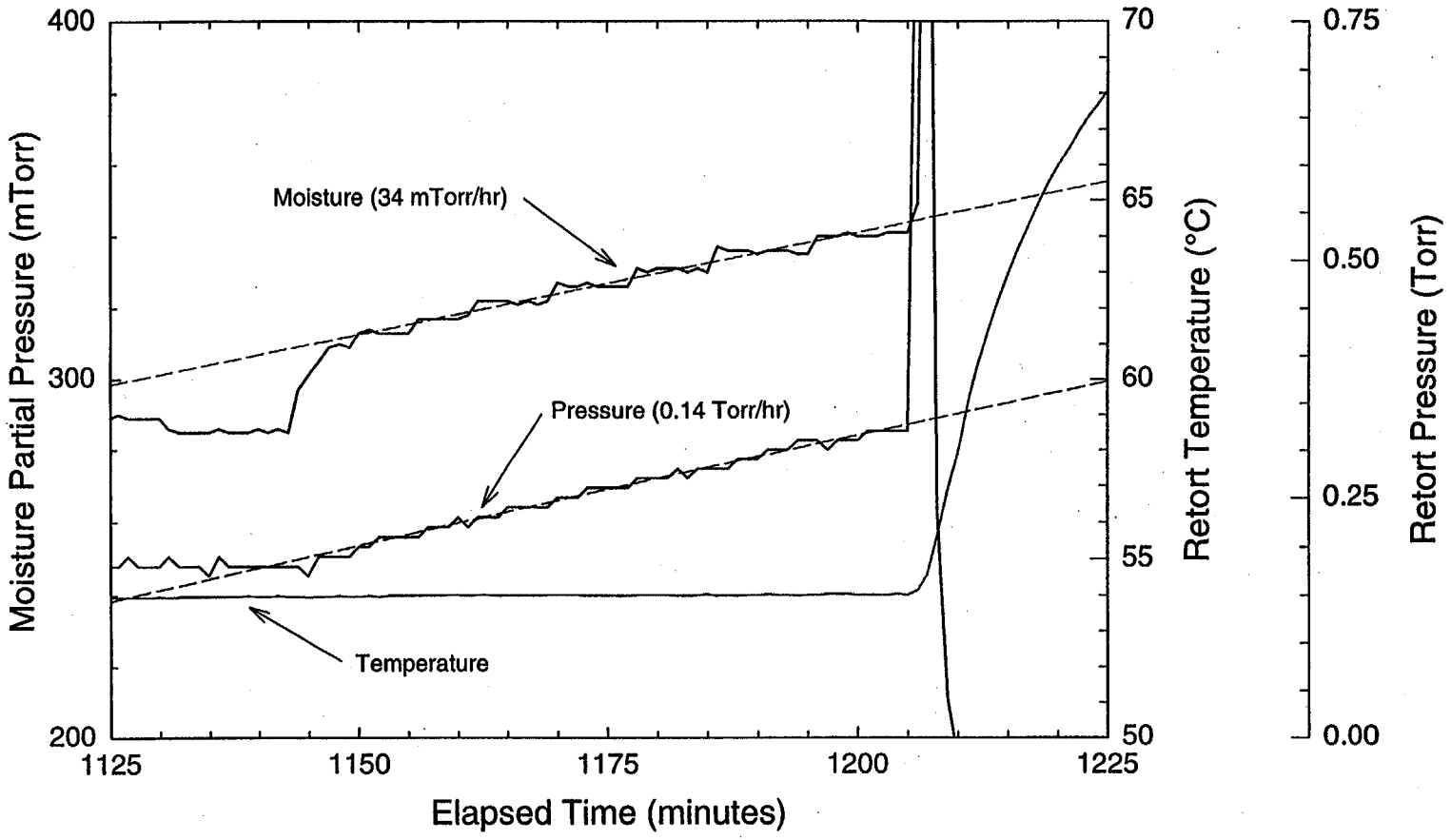

Figure 5.3. Drying of SNF Element 1164M, Post-CVD Pressure Rise Test

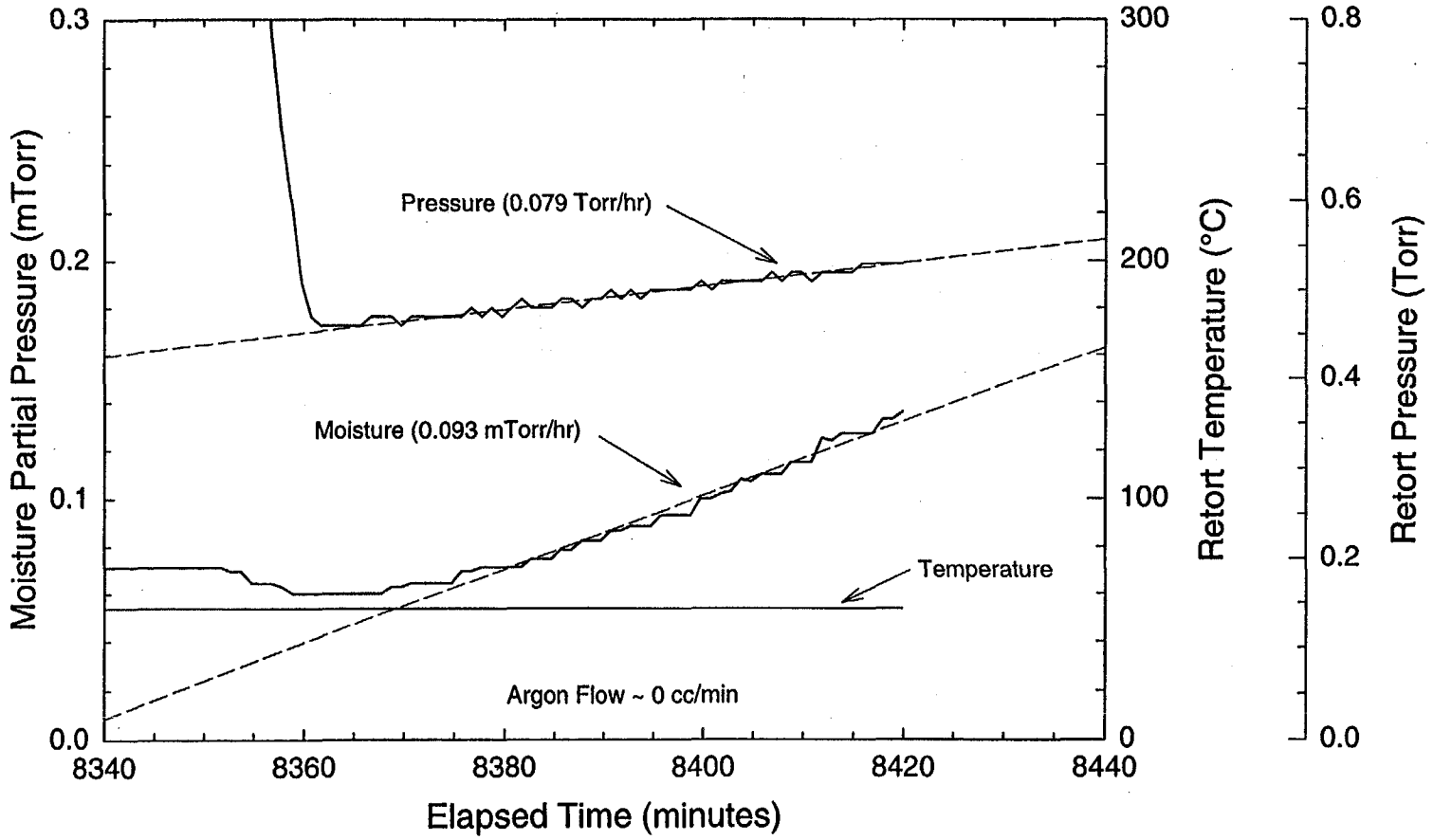

Figure 5.4. Drying of SNF Element 1164M, Post-HVD Pressure Rise Test

The post-CVD Pressure Rise Test was conducted over an ET of 1143 min to 1206 min. Both the total pressure and the moisture pressure showed nearly linear pressure rises over the course of the test. Regression fits (dotted lines in the figure) yielded a total pressure rise rate of ~0.14 Torr/hr (well below the 0.5 Torr/hr criterion for the test), and a moisture pressure rise rate of ~0.034 Torr/hr.

Assuming that the water vapor pressure increase is from water sources within the test system, and assuming ideal gas behavior of the water vapor, the rate of desorption of the water (dn/dt) will be constant, given by:

$$\frac{dn}{dt} = \frac{V}{RT} \cdot \frac{dP}{dt} \tag{5.1}$$

where n is the number of moles of gas, V is the volume of the system (~10,000 cm^3), R is the gas constant (82.06 $cm^3 \cdot atm/g\text{-}mol \cdot K$), T is the temperature (~326 K), and dP/dt is the rate of change in the pressure given by the slope of the regression line. The total amount of water released to the system during the Pressure Rise Test is given by the integral of the above equation. Assuming a total period of 63 min, the total amount of water released was ~0.4 mg. Assuming a total surface area of ~8900 cm^2 for the system (total surface area of the retort, sample boat, tubing, and an outer fuel element), and 10^{15} atoms per cm^2 as the monolayer gas density on surfaces, approximately two monolayer equivalents of H_2O were evaporated.

The results of the post-HVD pressure rise measurements are shown in Figure 5.4. Again, both the total pressure and the moisture pressure show essentially linear increases with time, however with significantly lower slopes than observed earlier for the post-CVD test. The total pressure rise has a regression slope of ~0.079 Torr/hr, and the moisture pressure rise has a slope of ~0.000093 Torr/hr. The rate of increase in the total pressure is similar to that observed in Runs 3 and 4, suggesting similar system sealing conditions.

As has been observed previously in Runs 4 and 5, the ratio of the water pressure rise to the total pressure rise is ~0.001, which is somewhat lower than would be expected just from humidity alone in air in-leakage from the cell environment (air at 20°C and 25% relative humidity would yield a water pressure-to-total pressure ratio of ~0.007). A likely explanation for the low moisture pressure rise in the post-HVD test is that the previous vacuum drying of the fuel element at temperature (during CVD and HVD) resulted in the formation of hygroscopic species, which "gettered" most of the moisture from either air in-leakage or from water remaining on the element that otherwise would have been released.

Comparison of the pressure data from two Pressure Rise Tests indicates that the total pressure rise observed in the initial post-CVD test is only partially caused by residual moisture and/or air in-leakage. The difference between the total pressure rise and the moisture pressure rise for the post-CVD test (~0.11 Torr/hr) is higher than can be explained by air in-leakage into the retort alone as measured in the post-HVD test. This suggests that other sources of gas, such as hydrogen, are responsible for some of the observed total pressure rise in the post-CVD test.

5.3 Hot Vacuum Drying

The first segment of HVD, shown in Figure 5.5, includes the ramp and hold from ~50°C to ~80°C in flowing argon gas (~324 cc/min) under partial vacuum. HVD-1 occurred over an ET of 1207 min to 2676 min. The moisture pressure decreased steadily from ~560 mTorr to ~4 mTorr during the ~80°C period. Total system pressure was essentially constant over this first HVD phase at ~19 Torr. Total water removed was ~0.7 g.

The second HVD phase involved maintaining the same system conditions as in HVD-1 but raising the temperature slowly from ~80°C to ~400°C at a rate of 10°C/hr. HVD-2 occurred over an ET of 2677 min to 4756 min, and is shown in Figure 5.6. During the temperature rise, the moisture pressure increased, showing three distinct peaks at ~130°C (~11 mTorr), ~176°C (~11 mTorr), and ~258°C (~6 mTorr). A smaller peak is possibly evident at ~360°C (~4 mTorr). These peaks are an indication of water release from chemisorbed sites (i.e., hydrated species) at higher temperatures. Total water removed during the second phase of HVD was ~0.2 g, approximately one third of that removed during the first phase. Total system pressure was essentially constant at ~19 Torr, except for a small rise of ~1 Torr at an ET of ~3800 min. As is discussed later, this rise in total pressure coincides with hydrogen release observed in both the GC and MS.

The third phase of HVD is shown in the left-hand side of Figure 5.7 (ET of 4757 min to 5222 min), and covered the temperature hold period at ~400°C. This period is characterized by a steady decrease in the moisture pressure from ~3 mTorr to ~0.2 mTorr. Total water removed was ~12 mg.

Following the final HVD phase, the system was allowed to cool to ~50°C in preparation for the post-test Pressure Rise Test discussed above. Water removed during the system cooldown was ~15 mg.

5.4 Gas Chromatograph Measurements

The GC was used to measure hydrogen in the sample gas during the HVD portion of the drying test when argon was flowing through the system. Argon flow also occurred during the initial portion of CVD, but the GC was not used. Hydrogen sampling during CVD is planned for Run 7. As discussed earlier, the hydrogen concentration data have been converted from ppmv to Torr·l so that the absolute quantity of hydrogen gas released can be determined independent of argon flow rate. To determine the location of the hydrogen peaks, and the integrated amounts of hydrogen involved with each peak, the hydrogen data were deconvoluted using a commercial peak fitting program, PeakFit. A five-parameter asymmetrical fitting function (Pearson IV) was used to fit each of the separate deconvoluted peaks.

Measured hydrogen release during the HVD segments of the drying test is shown in Figure 5.8. Three peaks are associated with the hydrogen release. The first occurred during the initial phase of HVD at ~75°C at an ET of ~1400 min. This peak was characterized by a fairly rapid rise in the hydrogen signal, followed by a slow, approximately exponential, decay. From deconvolution of the hydrogen data,

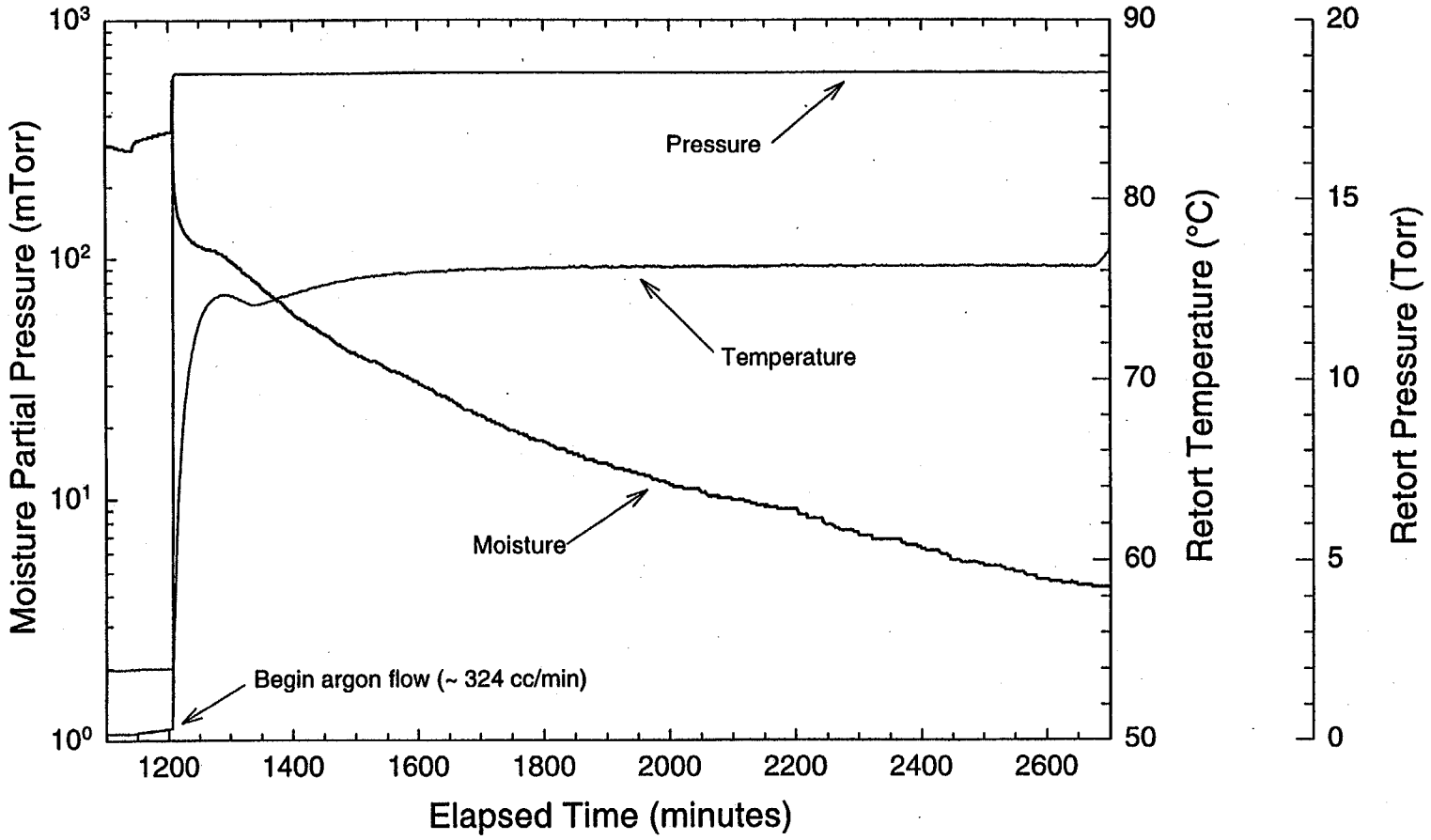

Figure 5.5. Drying of SNF Element 1164M, Hot Vacuum Drying – Step 1

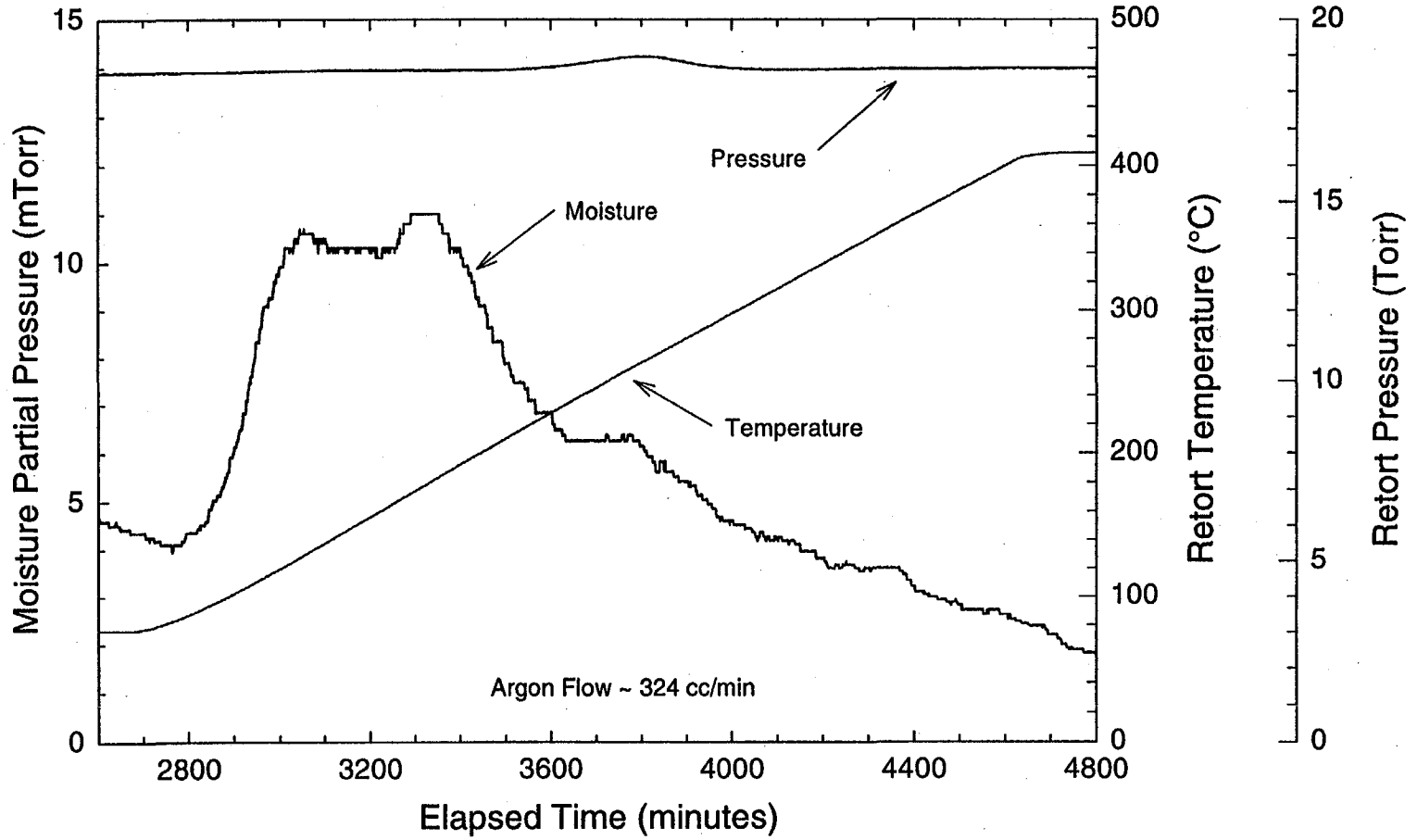

Figure 5.6. Drying of SNF Element 1164M, Hot Vacuum Drying – Step 2

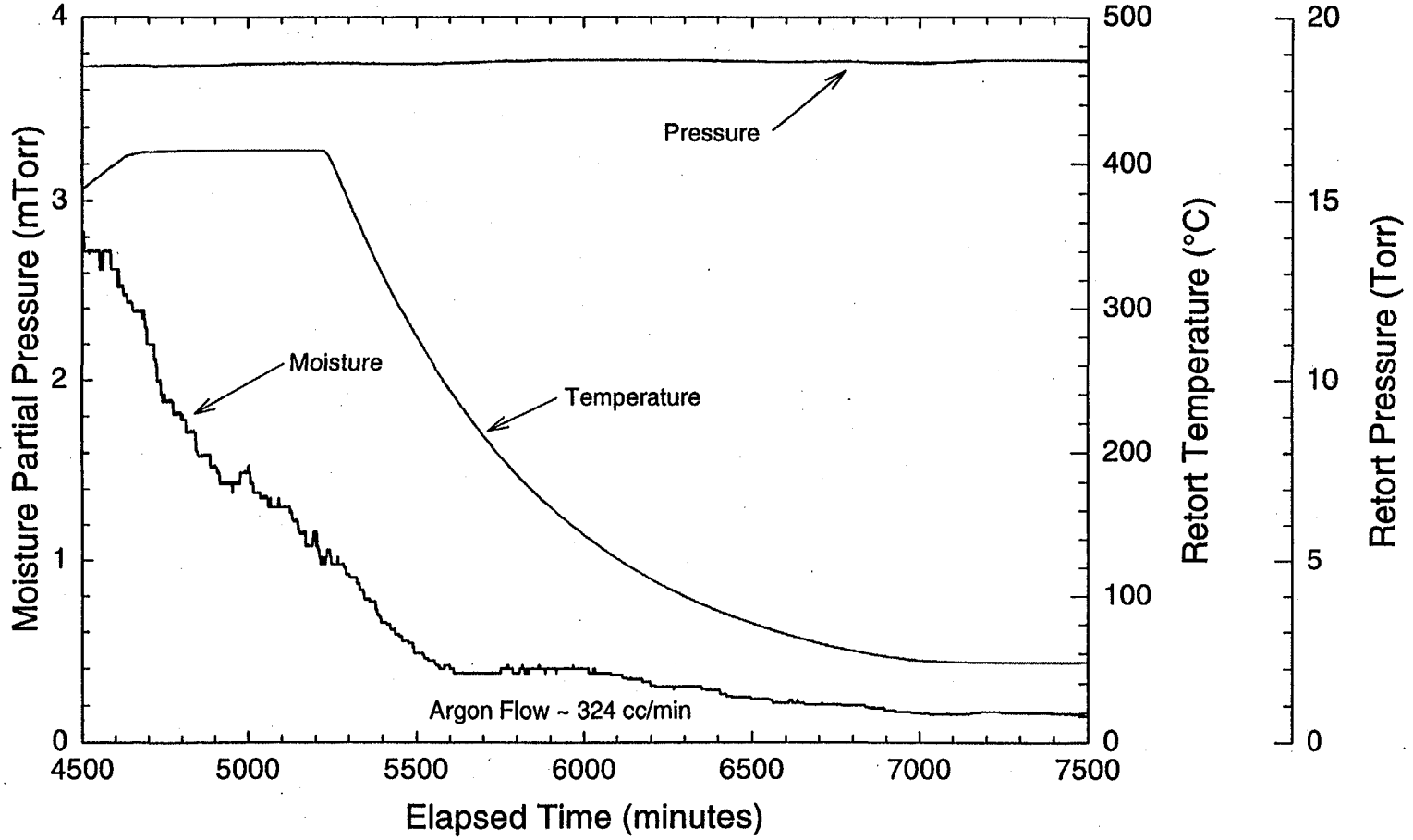

Figure 5.7. Drying of SNF Element 1164M, Hot Vacuum Drying – Step 3

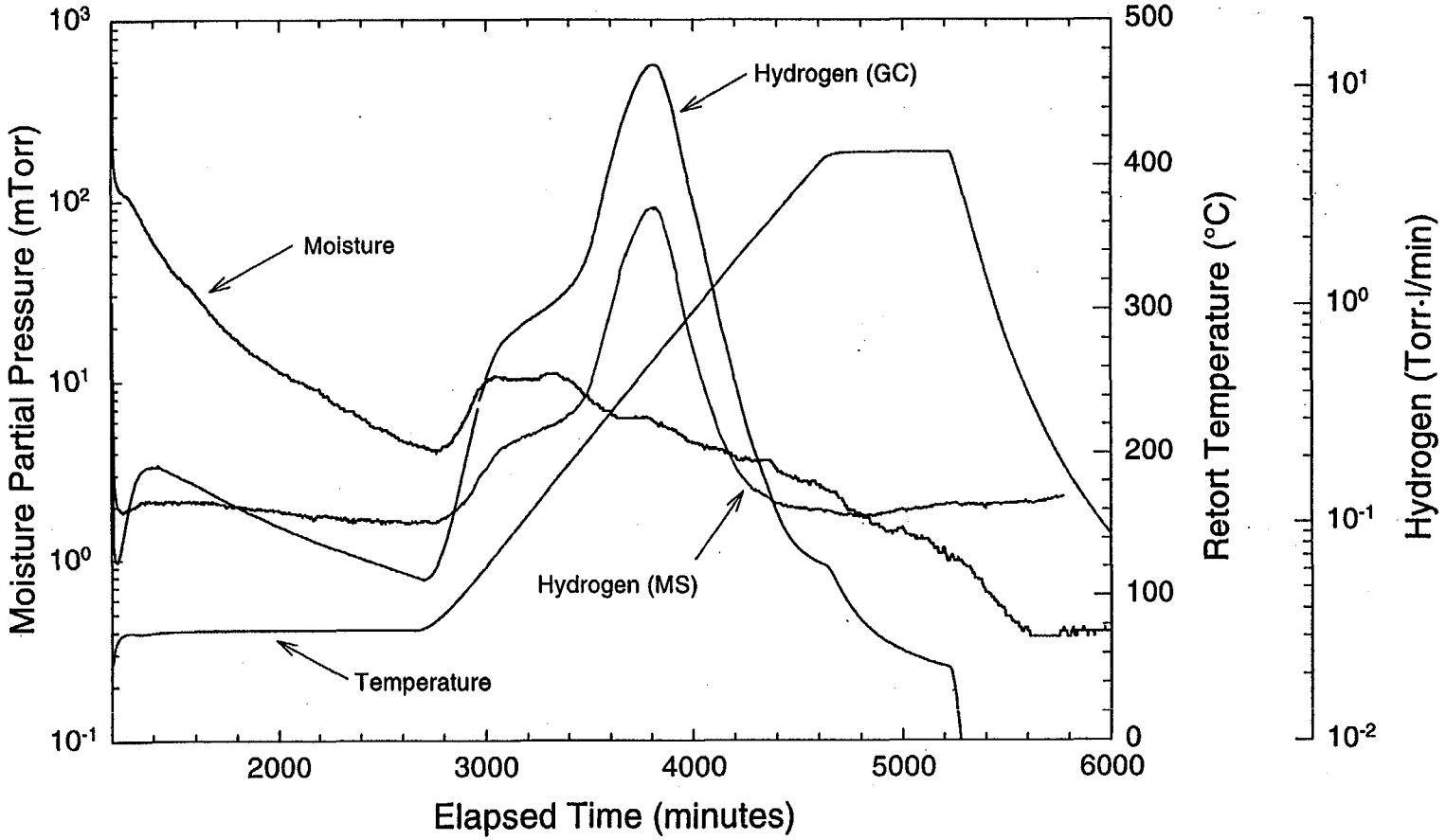

Figure 5.8. Drying of SNF Element 1164M, Hydrogen Release During HVD and Cooldown

~160 Torr·l (~17 mg) of hydrogen were released during HVD-1. The two remaining peaks occurred during HVD-2 at temperatures of ~155°C, and ~260°C. Approximately 4600 Torr·l (~500 mg) of hydrogen were released during the entire HVD process, over a time period of ~67 hr, with the majority being released during HVD-2.

As noted in Section 3.2.3, HVD-1 is isothermal, except for the initial temperature ramp from ~50°C to ~75°C, and can therefore be used to provide information on reaction kinetics. During HVD-1, the hydrogen signal first increases, and then later decreases steadily with time. By contrast, the water signal decreases steadily with time during HVD-1. This behavior has been observed in earlier runs and suggests that oxidation is occurring during the initial part of HVD-1 as the bulk of the fuel element reaches 75°C, with the oxidation slowing in the latter phases of HVD-1 in concert with the drop in available moisture. The 155°C peak during the early part of HVD-2 correlates closely with two water release peaks occurring at about the same time. Approximately 200 Torr·l (~22 mg) of hydrogen and ~96 mg of water were released during this time period. It is likely that the hydrogen released during this period was due to oxidation of fuel by water released through oxy-hydrate decomposition in the corrosion regions or in isolated regions under the cladding. As observed for the previous fuel element (6603M, Run 5), the molar ratio of water to hydrogen released was ~0.5, implying that water was reacting with the fuel at a faster rate than it was being released into the vacuum (and thus swept away with the argon flow past the moisture sensor).

The 260°C peak accounted for the majority of the hydrogen release, amounting to ~4200 Torr·l (~460 mg). This peak was most likely due to the decomposition of uranium hydride since there is little correlation with the water signal during this period, and also this temperature is close to the expected temperature for UH_3 decomposition (Cotton 1988). This quantity of hydrogen would represent ~37 g of UH_3 decomposition. The total quantity of hydrogen released during the HVD-2 phase was ~4500 Torr·l (~480 mg).

It should be noted that during the time in which hydrogen was being released from the decomposition of UH_3, the hydrogen concentration exceeded 50,000 appm. This concentration is about 50 times greater than the high-level standard (1050 appm) used to calibrate the GC. Although there was no evidence of signal saturation at this detection level, there is possibly some additional uncertainty in these higher-level hydrogen signals from nonlinearity in the GC instrument. For subsequent drying tests, the GC was configured to simultaneously collect data in both low and medium sensitivity ranges and, additionally, calibrated up to a level of 100,000 appm.

5.5 Mass Spectrometer Measurements

The Balzers Omnistar MS was used in conjunction with the GC to collect hydrogen and other gas release data over the test run. Hydrogen releases as measured by the GC are also shown Figure 5.8. As is evident, the MS hydrogen signal showed very similar trends as the GC data, with the magnitude of the peaks being somewhat smaller. This reduction in signal amplitude has been observed in previous drying runs, and is likely due to differences in the calibration pressure for the MS and the actual pressures encountered in these drying tests. Two modifications are planned to resolve this issue: 1) replacement of

the MS inlet pressure gauge with one that is more accurate in this low-pressure range, and 2) re-calibration of the MS at lower inlet pressures. These modifications will allow for more accurate normalization of the MS to actual sampling pressures.

Fission gases such as xenon were also measured by the MS during the test. Monitoring of these gases can be useful in categorizing individual hydrogen releases as being from oxidation of uranium by water or decomposition of uranium hydride. Measured ^{136}Xe releases during HVD are shown in Figure 5.9 along with the corresponding hydrogen and water release signals. For purposes of comparison, the ^{136}Xe data have been re-scaled and smoothed.

As can be seen in Figure 5.9, the general trends in the xenon release match similar trends in the water and hydrogen releases. Both the xenon and hydrogen releases show an initial signal increase followed by a slow decrease during the isothermal phase of HVD at ~75°C. Similarly, the xenon peak at ~3300 min corresponds closely with similar hydrogen and water release peaks at the same time. Both these trends further support oxidation of the fuel by released moisture during HVD-1 and the initial phase of HVD-2. The xenon peak at ~3900 min, however, is much narrower than the corresponding hydrogen peak, and is slightly delayed in time. Also, there is little evidence for any corresponding water release. This suggests that this xenon peak is likely from oxidation of newly exposed uranium surfaces resulting from hydride decomposition. A small amount of the xenon may have originated from the oxidation of the newly formed uranium from the hydride decomposition itself. This latter mechanism would be expected to be small, since most of the xenon would have been released from the uranium hydride during the original hydride formation.

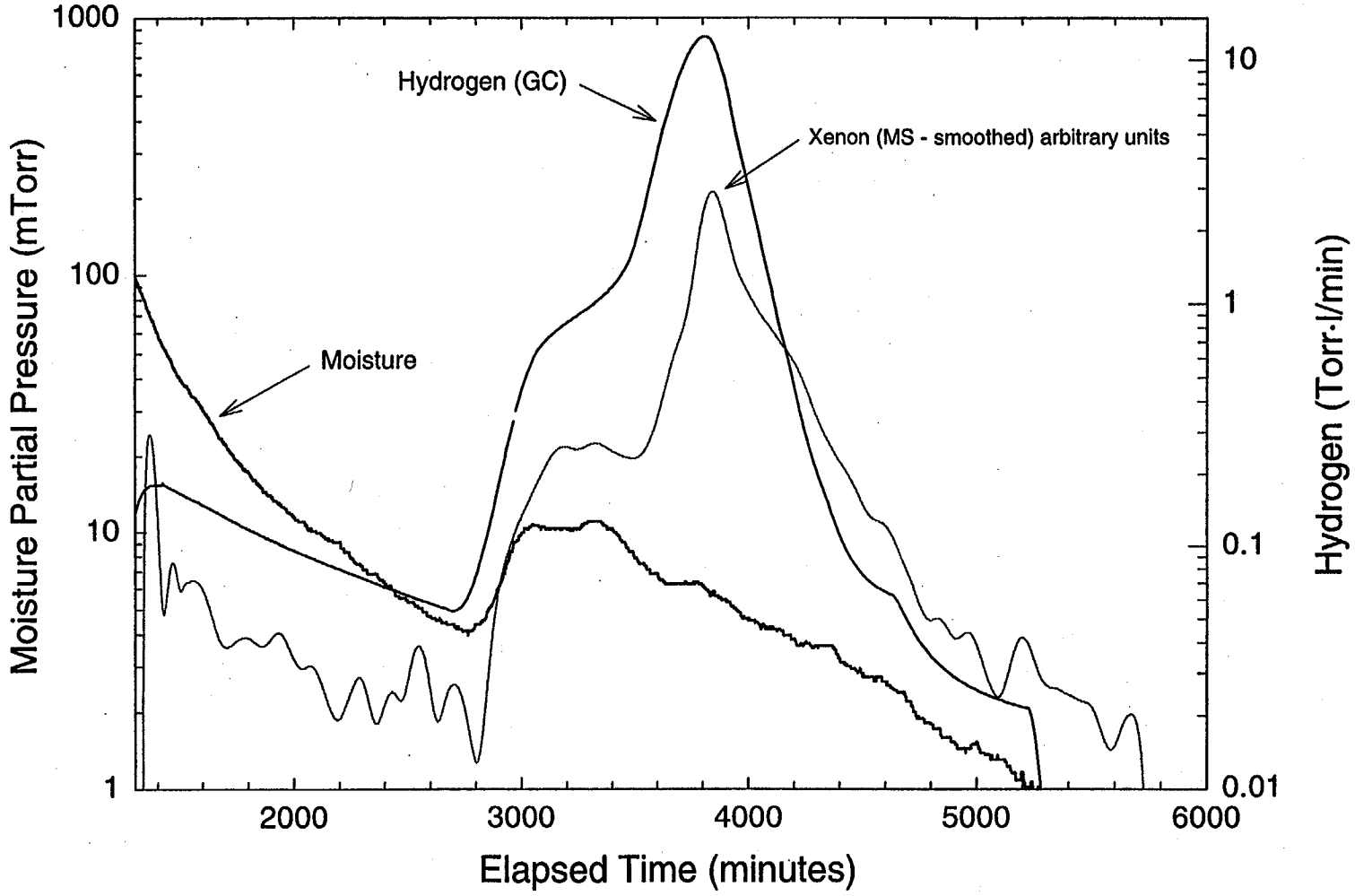

Figure 5.9. Drying of SNF Element 1164M, Normalized Xenon Release During HVD

6.0 Discussion

Approximately 5 ml of water were observed in the condenser during the condenser pumpdown phase of CVD, in close agreement with that calculated over the same time period. An additional ~0.4 mg of water was removed during the post-CVD Pressure Rise Test. As the temperature was only ~50°C, it is unlikely that metal oxy-hydrate decomposition was the source of this additional water. Therefore, this release can likely be interpreted as coming from free water that was trapped and not completely released during CVD. Similar to earlier tests, the total pressure rise observed in the post-CVD test was only partially caused by residual moisture, suggesting that other sources of gas are responsible for some of the total pressure rise observed in the post-CVD test.

During the first segment of HVD, approximately 0.7 g of water was removed at temperatures below ~80°C. The second phase of HVD released approximately 0.2 g of water with three main peaks at ~130°C, ~176°C, and ~258°C. The final phase of HVD at 400°C released only about 12 mg of water, with an additional ~15 mg of water released during post-HVD cooldown. This indicates that small residual quantities of water remained even after the drying test was completed. The total water observed or calculated to have been released during the drying run was ~6 g. The remaining water from the original quantity on the surface of the fuel element and from the added ~10 ml prior to CVD are assumed to have been removed by the scroll pump before and after the condenser phase, and by absorption and condensation in colder sections of the system such as the in-line filters.

Most of the water removal after the post-CVD Pressure Rise Test occurred during the first phase of HVD, which entailed the temperature ramp from ~50°C to ~80°C. This water release is attributed largely to the release of water from regions beneath the cladding and from under the corroded regions, although decomposition of metal oxy-hydrates may also account for some of it. Therefore, water released from the element from isolated regions along a "tortuous path" may be the controlling factor in post-CVD water removal. The peaks in the moisture release during HVD-2 indicate water release from chemisorbed sites (i.e., hydrated species) at higher temperatures. As observed in previous drying tests, a temperature above 400°C may be required for complete drying of the fuel element within a reasonable period of time.

Hydrogen data were obtained from the GC during HVD when argon was flowing through the system. Hydrogen was first observed starting at the ramp-up to ~75°C, reaching a peak at ~0.2 Torr·l before slowly decreasing. From deconvolution of the hydrogen data, ~160 Torr·l (~17 mg) of hydrogen were released during HVD-1, attributed to oxidation of the fuel by remaining free water. Hydrogen release increased again during the ramp from ~75°C to ~400°C, with two noticeable peaks at ~155°C and ~260°C, the first of which roughly corresponded to a similar water release and was ~200 Torr·l (~22 mg). It is likely that this hydrogen release is due to oxidation of fuel by water released through oxy-hydrate decomposition. The latter hydrogen release peak (~4200 Torr·l, or ~460 mg) at ~ 260°C is likely due to uranium hydride decomposition, and is equivalent to ~37 g of UH_3 decomposed. Above ~260°C, the level of hydrogen decreased rapidly with time, with ~13 Torr·l (~1.4 mg) of hydrogen released during HVD-3. Total hydrogen release during HVD was ~4600 Torr·l (~500 mg). The level of hydrogen release is the highest observed to date, tending to support the suggestion of a high effective surface area due to a

high degree of fuel fracturing. The level of hydrogen release is approximately six times that observed for the previous fuel element (6603M, Run 5).

Hydrogen data collected by the MS showed the same general trends as the GC data, but with the magnitude of the peaks being somewhat smaller. Xenon data from the MS during HVD correlated well with the water and hydrogen data during HVD-1 and the initial stages of HVD-2, supporting the argument that hydrogen release during this time period is due to oxidation of the fuel by water released through decomposition of oxy-hydrates. The xenon release, which occurred slightly after the large hydrogen release at ~260°C, suggests some oxidation of newly exposed uranium from hydride decomposition.

7.0 References

Cotton, F. A. 1988. *Advanced Inorganic Chemistry*, 5th Edition. John Wiley & Sons, New York.

CRC Press. 1997. *Handbook of Chemistry and Physics*, 78th Edition. New York.

Lawrence, L. A. 1997. *Strategy for Examination of the 15 K-West Basin Fuel Elements.* HNF-SD-SNF-SP-018, DE&S Hanford, Inc., Richland, Washington.

Ritter, G. A., S. C. Marchsman, P. J. MacFarlan, and D. A. King. 1998. *Whole Element Furnace Testing System.* PNNL-11807, Pacific Northwest National Laboratory, Richland, Washington.

Westinghouse Hanford Company (WHC). 1995. *Hanford Spent Nuclear Fuel Project Integrated Process Strategy for K Basins Spent Nuclear Fuel.* WHC-SD-SNF-SP-005, Rev. 0. Richland, Washington.

8.0 Supporting Documents and Related Reports

Gerry, W. M. 1997a. *Calibration of Mass Flow Controllers*. SNF-TP-012, Rev. 0, Pacific Northwest National Laboratory, Richland, Washington.

Gerry, W. M. 1997b. *Calibration of Balzer Quadstar Mass Spectrometer*. SNF-TP-014, Rev. 0, Pacific Northwest National Laboratory, Richland, Washington.

Gerry, W. M. 1997c. *Calibration of MTI Gas Chromatograph Model M200*. SNF-TP-013, Rev. 0, Pacific Northwest National Laboratory, Richland, Washington.

Serles, J. A. 1997. *Furnace Testing of N-Reactor Fuel Element 1164M*. PTL-007, Rev. 0, Pacific Northwest National Laboratory, Richland, Washington.

Reports are written separately for the whole element drying test series as follows:

System Design Description for the Whole Element Furnace Testing System

Spent Fuel Drying System Test Results (First Dry-Run)

Spent Fuel Drying System Test Results (Second Dry-Run)

Spent Fuel Drying System Test Results (Third Dry-Run)

Drying Results of K-Basin Fuel Element 1990 (Run 1)

Drying Results of K-Basin Fuel Element 3128W (Run 2)

Drying Results of K-Basin Fuel Element 0309M (Run 3)

Drying Results of K-Basin Fuel Element 5744U (Run 4)

Drying Results of K-Basin Fuel Element 6603M (Run 5)

Drying Results of K-Basin Fuel Element 1164M (Run 6)

Drying Results of K-Basin Fuel Element 2660M (Run 7)

Drying Results of K-Basin Fuel Element 6513U (Run 8)

Distribution

No. of
Copies

OFFSITE

C. L. Bendixsen
Idaho National Engineering and
Environmental Laboratory
P.O. Box 1625
Mail Stop 3135
Idaho Falls, ID 83415

A. W. Conklin
Washington State Department of Health
Airdustrial Park
Building 5, Mail Stop LE-13
Olympia, WA 98504-0095

M. A. Ebner
Idaho National Engineering and
Environmental Laboratory
P.O. Box 1625
Mail Stop 3114
Idaho Falls, ID 83415

A. R. Griffith
U.S. Department of Energy, Headquarters
19901 Germantown Rd (EM-65)
Germantown, MD 20585-1290

T. J. Hull
U.S. Department of Energy, Headquarters
19901 Germantown Road (EH-34)
Germantown, MD 20874-1290

M. R. Louthan
Savannah River Technology Center
Materials Technology Center
Aiken, SC 29808

No. of
Copies

T. E. Madey
Rutgers University
Bldg. 3865
136 Freylinghuysen Rd
Piscataway, NJ 08854

B. K. Nelson
U.S. Department of Energy, Headquarters
19901 Germantown Road (EM-65)
Germantown, MD 20874-1290

R. G. Pahl, Jr.
Argonne National Laboratory
P. O. Box 2528
Idaho Falls, ID 83403

R. S. Rosen
Lawrence Livermore National Laboratory
20201 Century Blvd., 1ST Floor
Germantown, MD 20874

D. Silver
Washington State Department of Ecology
P.O. Box 47600
Olympia, WA 98504-7600

T. A. Thornton
Yucca Mountain Project M&O Contractor
SUM1/423
1261 Town Center Drive
Las Vegas, NV 89134

No. of Copies

ONSITE

6 DOE Richland Operations Office

R. M. Hiegel	S7-41
P. G. Loscoe	S7-41
C. R. Richins	K8-50
E. D. Sellers	S7-41
J-S. Shuen	S7-41
G. D. Trenchard	S7-41

24 Duke Engineering and Services, Hanford, Inc.

C. B. Aycock	R3-11
R. B. Baker	H0-40
D. W. Bergmann	X3-79
S. A. Chastain	H0-40
D. R. Duncan	R3-86
J. R. Frederickson	R3-86
L. H. Goldmann	R3-86
S. L. Hecht	HO-40
L. A. Lawrence (5)	H0-40
P. J. MacFarlan	H0-40
B. J. Makenas	H0-40
R. P. Omberg	H0-40
R. W. Rasmussen	X3-85
A. M. Segrest	R3-11
J. A. Swenson	R3-11
C. A. Thompson	R3-86
D. J. Trimble	H0-40
D. J. Watson	X3-79
J. H. Wicks, Jr.	X3-74
SNF Project Files	

3 Fluor Daniel Hanford

E. W. Gerber	R3-11
D. A. Smith	T4-13
M. J. Wiemers	R3-11

No. of Copies

2 Fluor Daniel Northwest

L. J. Garvin	R3-26
G. A. Ritter	H0-40

7 Numatec Hanford Company

G. P. Chevrier	H5-25
T. Choho	R3-86
E. R. Cramer	H0-34
T. A. Flament	H5-25
J. J. Irwin	R3-86
C. R. Miska	R3-86
J. P. Sloughter	H5-49

COGEMA Engineering Corporation

A. L. Pajunen	R3-86

2 Technical Advisory Group

J. C. Devine	R3-11
R. F. Williams	R3-11

32 Pacific Northwest National Laboratory

J. Abrefah	P7-27
J. P. Cowin	K8-88
S. R. Gano	K2-12
W. J. Gray	P7-27
B. D. Hanson	P7-27
G. S. Klinger	P7-22
D. K. Kreid	K7-80
J. M. Latkovich	K9-44
S. C. Marschman (10)	P7-27
B. M. Oliver (5)	P7-22
T. M. Orlando	K8-88
J. C. Wiborg	K7-74
Information Release (7)	